PSDC-TR-16

Supplement No. 1

AN EXPERIMENTAL EVALUATION OF ROOF REDUCTION FACTORS WITHIN A MULTI-STORY STRUCTURE

by
R. Spring
C. H. McDonnell

April 1967

for
Office of Civil Defense

by
The CONESCO Division of Flow Corporation

Contract DACA 31-67-C-0018
OCD Sub Task 1117 A

through

PROTECTIVE STRUCTURES DEVELOPMENT CENTER
Joint Civil Defense Support Group
Office of Chief of Engineers
Department of the Army
Washington, D.C. 20315

SUMMARY

PSDC-TR-16
Supplement No. 1

AN EXPERIMENTAL EVALUATION OF ROOF REDUCTION FACTORS

April 1967

Technical Report Prepared for

Office of Civil Defense
Office of the Secretary of the Army
Washington, D.C. 20310

By

CONESCO, A Division of Flow Corporation
Watertown, Massachusetts
Contract DACA 31-67-C-0018
Work Order (OCD) DAHC20-67-W-0111
Subtask 1117A

Through

The Protective Structures Development Center
Joint Civil Defense Support Group
Fort Belvoir, Virginia

Fallout contamination deposited on the roof of a structure is, in many cases, the source of the primary radiation component of the total dose obtained at any point within the structure. Experiments have been performed in which the doses from a source of radiation present on a roof were measured in many locations within a multi-story building.

This report presents the results of these experiments for roof and floor mass thicknesses of 48.6 and 97.2 psf. Comparisons of the experimentally measured gamma doses with those determined theoretically have been shown throughout this report. Agreement between experiment and theory has, in general, been found to be good.

PSDC - TR - 16
Supplement No. 1

AN EXPERIMENTAL EVALUATION OF ROOF REDUCTION FACTORS WITHIN A MULTI-STORY STRUCTURE

by

R. Spring

and

C. H. McDonnell

April 1967

Prepared by

The CONESCO Division of Flow Corporation
under Contract DACA 31-67-C-0018
Work Order No. OCD Sub Task 1117A
(OCD) DAHC20-67-W-0111

Report No. PSDC-TR-16 Supplement No. 1

Report to
Office of Civil Defense
from

Protective Structures Development Center
Joint Civil Defense Support Group
Office of Chief of Engineers/ Naval Facilities Engineering Command
Washington, D.C.

SUMMARY

Fallout contamination deposited on the roof of a structure is, in many cases, the source of the primary radiation component of the total dose obtained at any point within the structure. Experiments have been performed in which the doses from a source of radiation present on a roof were measured in many locations within a multi-story building.

This report presents the results of these experiments for roof and floor mass thicknesses of 48.6 and 97.2 psf. Comparisons of the experimentally measured gamma doses with those determined theoretically have been shown throughout this report. Agreement between experiment and theory has, in general, been found to be good.

FOREWORD

This report presents results of an experimental evaluation of radiation attenuation and distribution caused by simulated fallout from the roof of a multi-story structure with floors of varying mass thicknesses. The experiment was performed during the period August 1965-1966 by the CONESCO Division of Flow Corporation at the Protective Structures Development Center (PSDC), Fort Belvoir, Virginia.

This work was conducted for the Office of Civil Defense through the PSDC, Joint Civil Defense Support Group (JCDSG), Office of the Chief of Engineers, and was accomplished under Subtask 1117A Contract DA-18-050-ENG-3407, Work Order No. OCD-PS-65-17 and Contract DACA 31-67-C-0018, Work Order No. (OCD) DAHC 20-67-W-0111.

Mr. R.F. Stellar is Chief of the JCDSG and Mr. M.M. Dembo is Chief of its PSDC element. All Conesco operations under this contract come under their supervision.

Prior work is reported in PSDC-TR-14, "Description, Experimental Calibration, and Analysis of the Radiation Test Facility at the Protective Structures Development Center," PSDC-TR-15, "The Barrier Attenuation Introduced by a Vertical Wall," and PSDC-TR-16, "An Experimental Evaluation of Roof Reduction Factors."

The authors wish to express their appreciation to all who participated in this experiment. In particular, they wish to asknowledge the contributions of:

Mr. D.S. Reynolds and Mr. George Ploudre of the PSDC Staff, who assisted in the experiments, supervised logistical support required for the accomplishment of the tests, and monitored the work for the Government; and

Mr. Charles Eisenhauer, National Bureau of Standards and Mr. John Batter of CONESCO, who supported this study by their consultations and technical suggestions.

Mr. John Dardis, U.S. Naval Radiological Defense Laboratory, who provided a technical review of this report.

CONTENTS

LIST OF ILLUSTRATIONS

LIST OF TABLES

NOMENCLATURE

A	=	area of contaminated field (ft^2)
C	=	charger-reader calibration constant
D	=	total dose-roentgens
D_o	=	infinite field 3 ft. dose rate
e	=	eccentricity of structure (W/L)
H	=	height of source above ground (ft.)
I	=	specific dose rate (R/hr)/(curie/ft^2)
L	=	building length
$\ell(d,\cos\theta)$	=	differential angular distribution of dose
$L(X)$	=	the total detector response at a mass thickness, X, from an infinite, plane isotropic source, divided by the total detector response at 3 feet in air from the same source
L_a	=	attenuation introduced by a barrier adjacent to the source plane
L_b	=	attenuation introduced by a barrier adjacent to the detector
L_c	=	attenuation introduced by a barrier uniformly distributed between source and detector
m	=	charger-reader microamp scale reading
n	=	$2Z/L$
p	=	pressure (in. of Hg)
R_f	=	reduction factor = I/D_o
S_o	=	source strength in curies
$S(X,\cos\theta)$	=	attenuation of parallel monodirectional radiation
T	=	temperature in degrees Rankine
t	=	time (hr)
W	=	building width

X	=	effective mass thickness of barrier (psf)
Z	=	source-to-detector distance
θ	=	polar angle measured relative to a perpendicular from the detector to the source plane
ω	=	solid angle fraction

CHAPTER 1
INTRODUCTION

As part of a continuing experimental program designed to verify the theoretical methods utilized in computing the dose rates within a structure from contamination lying on the roof, the CONESCO Division of the Flow Corporation has conducted experiments using a multi-story, concrete structure. The results of these experiments and their comparison with calculated values are presented in this report.

The initial phase of the roof analysis program was restricted to experiments performed on a single-story structure, thus concentrating the barrier near the source of radiation. The second phase of the program, in which floors were placed within the structure, provided experimental data which were compared with results obtained from analytical methods[1] in which the attenuating barrier was distributed between the source and the detector.

This method[1], in its current form, treats barrier masses interposed between roof sources and detectors as being uniformly distributed in space. The authors of this method have assumed that this treatment is more representative of the actual situation than if the attenuating mass had been concentrated at either the source or detector locations.

CHAPTER 2

THEORETICAL BACKGROUND

2.1 CALCULATIONAL METHODS

In the analysis of structural shielding from nuclear fallout, photon attenuation by a roof is presented in terms of a reduction factor. The reduction factor is defined as the ratio of the dose at any location from a contaminated area of arbitrary geometry to the dose encountered at a point 3 feet in the air above an infinite, smooth, uniformly contaminated plane of similar density.

Spencer[2], from a purely theoretical solution of the transport equation in an infinite media, has developed three functions representing different assumptions regarding barrier placement that are to be employed as approximations to roof reduction factors. Each of these functions is dependent on X, the barrier mass thickness, and ω, the fraction of the solid angle subtended at the detector by a circular source field. It is tacitly assumed that both a rectangular plane and a circular source plane yield identical reduction factors when viewed as functions of a solid angle fraction. The validity of this assumption in the case of the barrier concentrated near the source has been adequately demonstrated experimentally for the case of a roof with a 1.5 length-to-width ratio in previous work.[3]

The three functional expressions developed by Spencer are pictorially represented in Figure 2.1. Each expression represents a slightly different geometric situation. A detailed analysis of the functions has previously been presented[2,3] and is thus only outlined briefly here. The expressions are utilized to represent three different source-barrier-detector configurations; viz., (1) the barrier concentrated near the source; (2) the barrier concentrated near the detector; and (3) the barrier uniformiy distributed between source and detector. The functions are labelled, respectively, $L(X)\,L_a(X,\omega)$, $L(X)\,L_b(X,\omega)$, and $L(X)\,L_c(X,\omega)$ expressed in terms of a roof reduction factor. The term L(X) is defined[2] as the total detector response beyond a barrier thickness X from an infinite plane, isotropic source divided by the total detector response at 3 feet in the air from the same source.

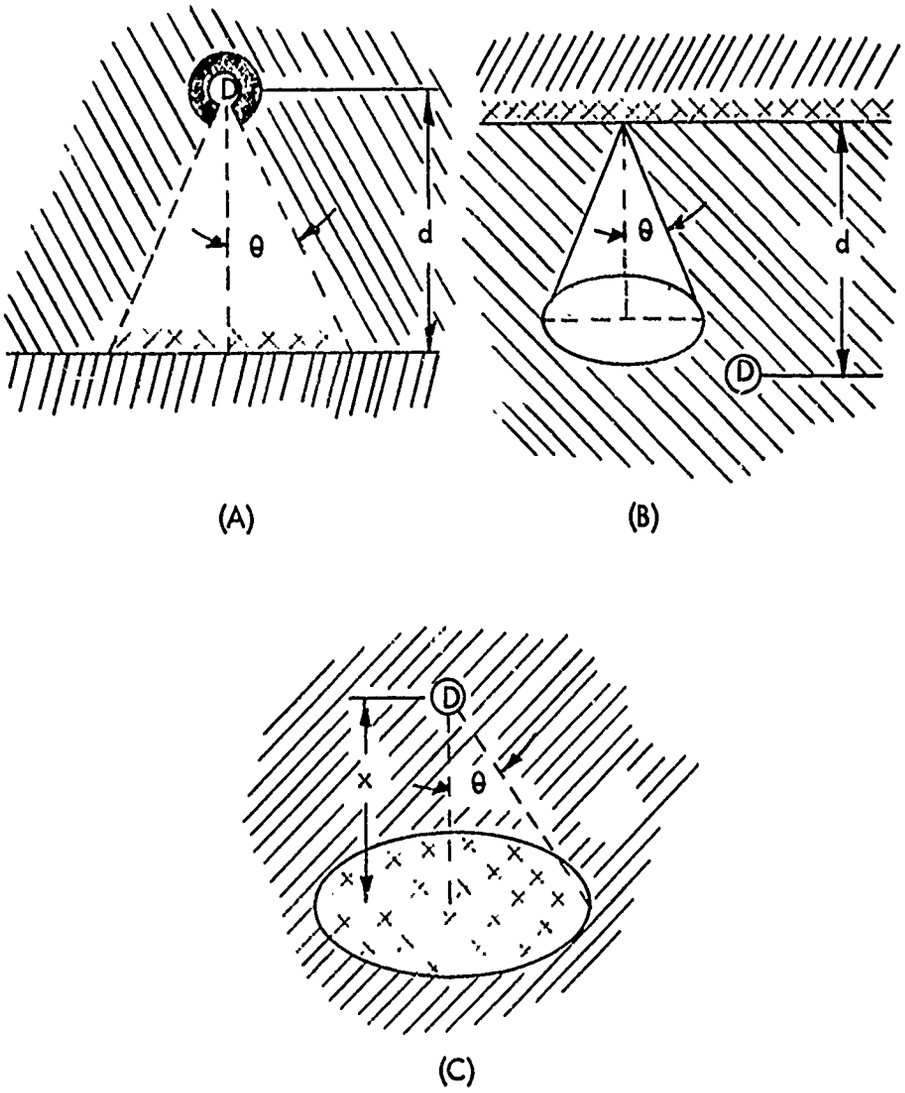

$$\omega = 1 - \cos\theta$$

FIG. 2.1 - DETECTOR-SOURCE-MEDIUM ARRANGEMENTS

2.2 MASS NEAR SOURCE

The function $L_a(X, \omega)$ represents the reduction in detector response which occurs if an isotropic detector, separated from an infinite plane source of gamma rays by a barrier thickness X, is replaced by a detector responding only to gamma rays incident within a particular cone of directions (Figure 2.1a). Note that this is analogous to the attenuating mass being concentrated next to the source, because, in this situation, the attenuating mass defines the solid angle. The function is expressed in terms of the differential dose angular distribution as follows:

$$L_a(X, \omega) = \frac{\int_{\cos\theta}^{1} \ell(X, \cos\theta)\, d(\cos\theta)}{\int_{-1}^{1} \ell(X, \cos\theta)\, d(\cos\theta)} \qquad (2.1)$$

where

$\omega = 1 - \cos\theta$ is the solid angle fraction of the source field as viewed by the detector,

$\ell(X, \cos\theta)$ = the dose angular distribution at mass thickness X above an infinite plane source of contamination immersed in an infinite medium, and

$d(\cos\theta)$ = the differential incremant of the solid angle.

2.3 MASS NEAR DETECTOR

A second estimation of the dose resulting from a limited area of contamination is $L_b(X, \omega)$. This function expresses a fractional reduction in detector response which occurs if an infinite plane isotropic source is suddenly constricted to emitting radiation only into a limited cone of directions about the perpendicular toward the detector (Figure 2.1b). This situation is approximately equivalent to concentrating the barrier at the detector as photons arriving at large angles find it increasingly difficult to penetrate the large slant distances through the barrier. This function is expressed as:

$$L_b(X, \omega) = v \frac{\int_{1-\omega}^{1} s(X, \cos\theta)\, d(\cos\theta)}{\int_{-1}^{1} \ell(X, \cos\theta)\, d(\cos\theta)} \qquad (2.2)$$

where

$s(X, \cos\theta)$ = the attenuation provided by a slab of thickness X from the face of the slab which is irradiated by parallel, monodirectional gamma rays of incident obliquity θ;

v = a proportionality constant so that integration over all obliquities will give the plane source isotropic source results;

$\ell(X, \cos\theta)$ = the dose angular distribution at mass thickness X above an infinite plane source of contamination immersed in an infinite medium.

2.4 MASS DISTRIBUTED BETWEEN SOURCE AND DETECTOR

The expression $L_c(X, \omega)$ is the ratio of the response of an isotropic detector caused by a circular area of contamination to that caused by an infinite plane, isotropic source of gamma radiation (Figure 2.1c). Its analytical expression is developed from the equations for dose above an infinite plane field of contamination, and for the dose above the same plane containing a cleared circular area centered below the detector. These equations are identical and a function only of the slant distance from the detector to the edge of the cleared circle. The dose rate at height X (equivalent mass thickness) above an infinite field of contamination is computed as:

$$L(X) = \int_{-1}^{1} \ell(X, \cos\theta)\, d(\cos\theta) \qquad (2.3)$$

with quantities as previously defined. The dose rate above an infinite plane source of contamination containing a cleared circle subtending

angle θ below the detector is expressed as:

$$L\left(\frac{X}{\cos\theta'}\right) = \int_{-1}^{1} \ell\left[\left(\frac{X}{\cos\theta'}\right), \cos\theta\right] d(\cos\theta) \qquad (2.4)$$

By subtraction, the dose rate from a circular area of contamination of cone angle θ' as viewed by the detector is:

$$L_c(X,\omega) = \frac{1}{L(X)}\left[L(X) - L\left(\frac{X}{\cos\theta'}\right)\right] \qquad (2.5)$$

Roof dose measurements in a multi-story structure have been considered to be best represented by the $L(X)\,L_c(X,\omega)$ function, since the barrier is generally located in finite layers between the source and detector. This function partially accounts for the radiation from an isotropic source which has been scattered to the detector from outside the solid angle subtended by the source plane.

2.5 CALCULATIONAL ERRORS

Spencer[2] estimates that errors in the calculations caused by truncation of the moments solutions and the correspondingly required smoothing of the angular distribution used in calculating $L_a(X,\omega)$, $L_b(Y,\omega)$, and $L_c(X,\omega)$ range between 0 and 25 percent. On the other hand, in the $L(X)$ calculations, the error caused by moment truncation alone reaches a maximum of about 5 percent. Errors caused by inaccurate input information (about 5 percent), errors inadvertently introduced when drafting the graphs, and those caused by the procedures for using the data must be added to these estimates. This latter error is traceable to the inadequacies of the schematization which is, in part, evaluated in this study.

2.6 SOLID ANGLE FRACTIONS

As previously mentioned, it is often useful to represent roof reduction factors as functions of solid angle fractions. The solid angle fraction is defined as the solid angle subtended by the source plane at the detector divided by 2π. For a circular source plane, the solid angle fraction

is given as:

$$\omega = \frac{1}{2\pi} \int \frac{\cos\theta \; dA}{r^2} = \int d(\cos\theta) = 1 - \cos\theta_o \quad (2.6)$$

where θ is the angle between the normal to the center of the disk and a line drawn from the detector to any point on the disk (Figure 2.2).

In reality, however, most roofs are best represented by rectangular areas. The calculated values of the roof reduction factors were developed for a circular geometry and the assumption is implicitly made that the detector response is equivalent from a circular disk source and a rectangular source subtending the same solid angle. The solid angle fraction below a rectangle is represented by

$$\omega = \frac{2}{\pi} \tan^{-1} \left[\frac{e}{n\sqrt{n^2 + e^2 + 1}} \right] \quad (2.7)$$

here

e = ratio of length to width of rectangle

n = perpendicular distance from detector to rectangle divided by half of the length of the rectangle.

2.7 PREVIOUS WORK IN THIS FIELD

The preceding PSDC report on roof attenuation[3] briefly commented on studies previously completed on this subject. These include work by Eisenhauer,[4] Raso,[5] Clarke,[6] Titus,[7] Batter,[8] and Schmoke[9]. These experiments were conducted in single-story structures and hence are not directly comparable with this work except on the third floor where good agreement was achieved with the $L(X)\, L_a\, (X, \omega)$ function. The experiment reported herein is believed to be the first detailed study conducted on a full scale, multi-story building.

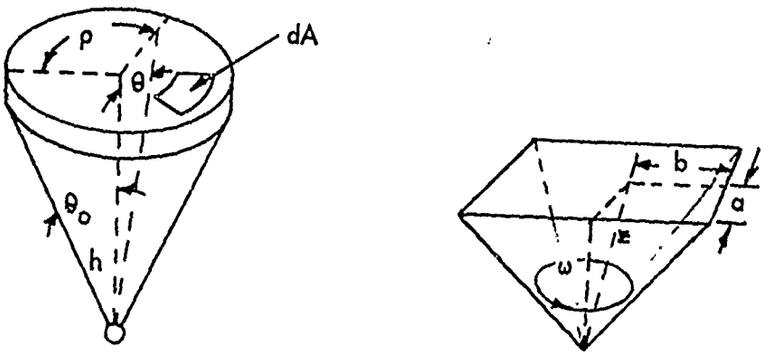

$$e = a/b$$

$$n = z/b$$

$$\omega = (2/\pi)\left(\mathrm{Tan}^{-1}\left\{\frac{e}{n\sqrt{n^2 + e^2 + 1}}\right\}\right)$$

FIG. 2.2 - SCHEMATIC DIAGRAM FOR SOLID ANGLE FRACTION CALCULATIONS

CHAPTER 3

EXPERIMENTAL ARRANGEMENT AND RESULTS

3.1 BACKGROUND

Experiments to determine the attenuation of gamma rays from simulated fallout by the roof of a structure have been performed at the Protective Structures Development Center. Several structural geometries have been investigated in the course of this program so that the calculational methods outlined in the OCD PM-100-1[1] might be fully evaluated. The first phase[3] of this program, was primarily concerned with single-story structures. In that phase the dose rates were measured below a source of radiation on the roof of a box-type structure (consisting of four walls and a roof with no floors or partitions) and compared with existing theory. In the second phase of the study (described in this report), floors were introduced in the structure, thereby producing a three-story building. Dose rates were then measured below the roof source on each of the stories. The third phase, and last of the overall roof program, will retain the floors in the structure and introduce interior partitions on each floor. This phase will be reported separately.

The experimental test structure and the method of obtaining a simulated fallout radiation field have been described in detail in a previous report[10] and hence are only described briefly in this report.

3.2 SOURCE OF RADIATION

To create a simulated field of contamination on the roof of the structure, a sealed Co-60 source was pumped at a constant velocity through a length of polyethylene tubing pre-arranged to simulate contamination uniformly covering the particular geometrical configuration of interest. In the present experiments, two geometries were investigated: (1) a full roof source, i.e., a rectangle 24 feet wide by 36 feet long; and (2) a circular disk source 11.5 feet in diameter. Figure 3.1 illustrates the placement of the tubing arrangement on the roof for each of the above situations. The smaller area disk source was utilized to produce test results for smaller values of the solid angle fraction than was possible with the full rectangular roof source.

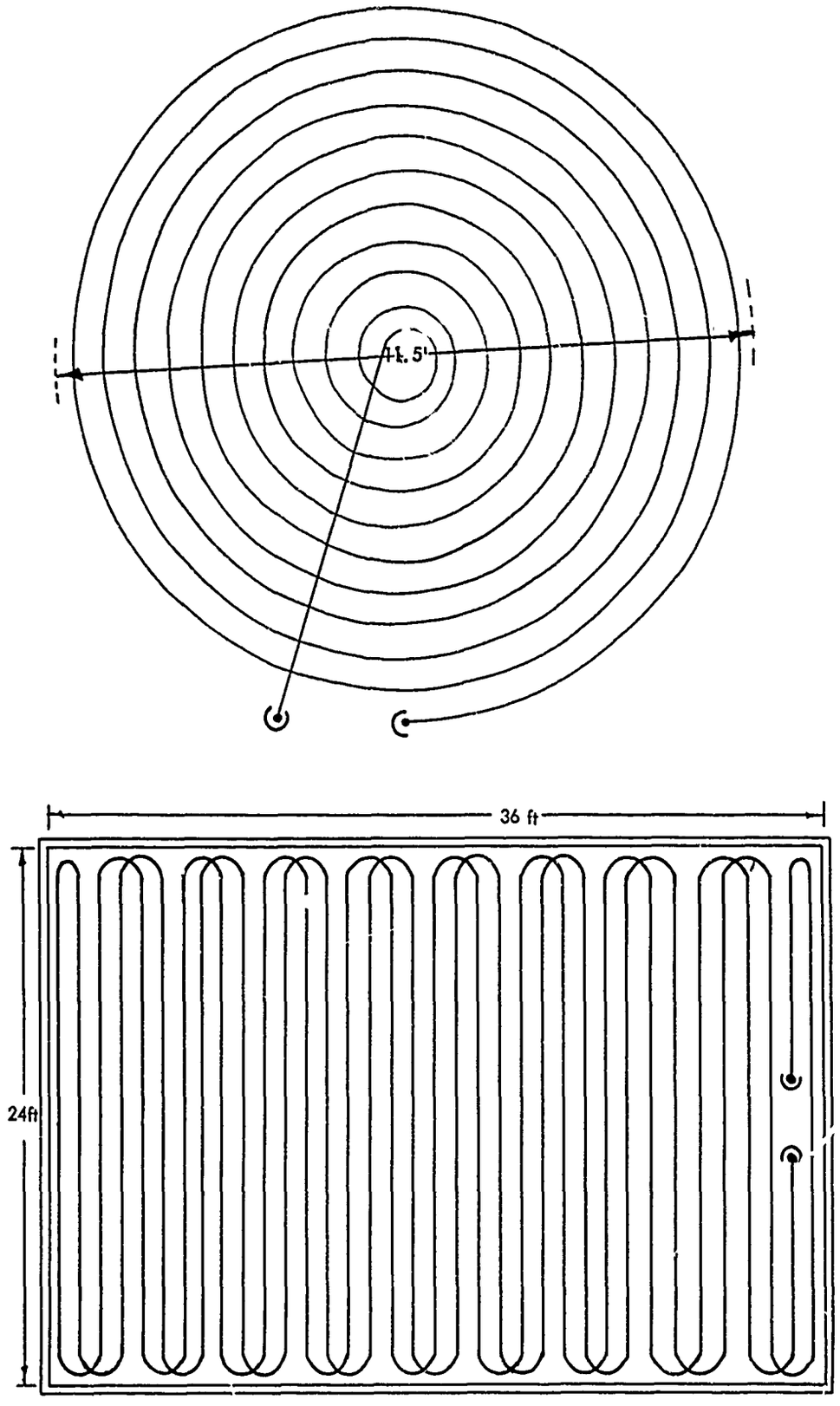

FIG. 3.1 Tubing Layout For Rectangular and Circular Roof Contamination

3.3 TEST STRUCTURE

The experimental test structure was composed of a steel skeleton supporting concrete panels as walls and floors. Figure 3.2 and 3.3 show the test structure with and without the concrete panels. The interior dimensions of the building were 24 feet in width by 36 feet in length by 36 feet in height. The bottom face of the floor slabs were positioned at 11-, 23-, and 35-foot elevations. For the experiments described in this report, the walls of the test structure remained at a constant thickness of 4 inches. Two roof and floor thicknesses were investigated; viz., 4 inches (48.6 psf) and 8 inches (97.2 psf).

3.4 DETECTOR POSITIONS

In the experiments in which the disk source of radiation was utilized on the roof, measurements of the dose within the structure were made only along the axis intersecting the center of the disk. Since the disk was positioned in the center of the rectangular roof, this axis corresponded to the centerline of the test structure. For the full roof source, measurements were made not only along this centerline, but also at various symmetric off-center locations. A floor plan of the test structure illustrating the center and off-center dosimeter locations is shown in Figure 3.4.

3.5 ACCURACY OF EXPERIMENTAL DATA

To determine the accuracy of the data obtained from the roof experiments, the errors or uncertainties of many parameters had to be considered. Since it was impractical to determine experimentally all of the uncertainties associated with weather, exposure time, source strength, and so forth, in a completely rigorous way, it was necessary to estimate some of the errors and uncertainties from practical experience. A detailed analysis of those errors is presented in Appendix B. By compounding these values according to accepted principles, the standard deviation of error was determined and is presented in Table 3.1.

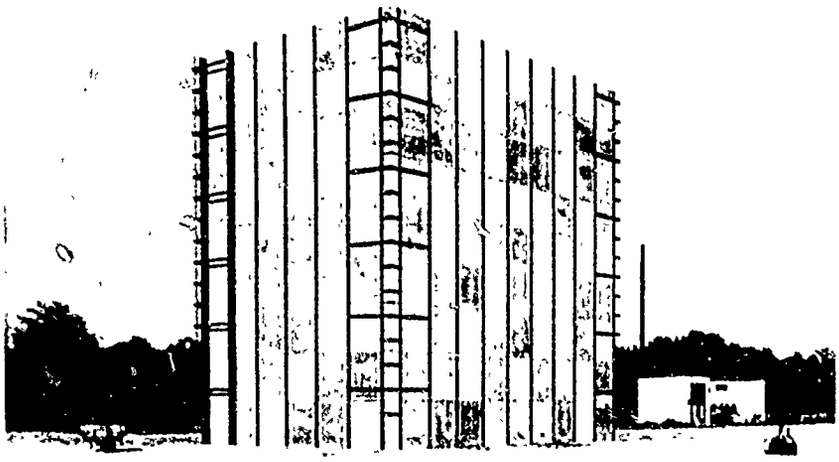

Photograph of

Figure 3.2 Assembled Test Structure

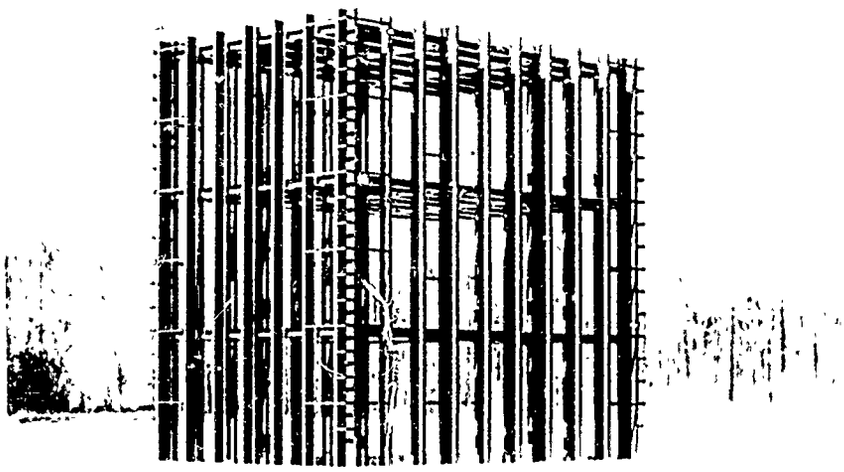

Photograph of

Figure 3.3 Steel Frame of Test Structure

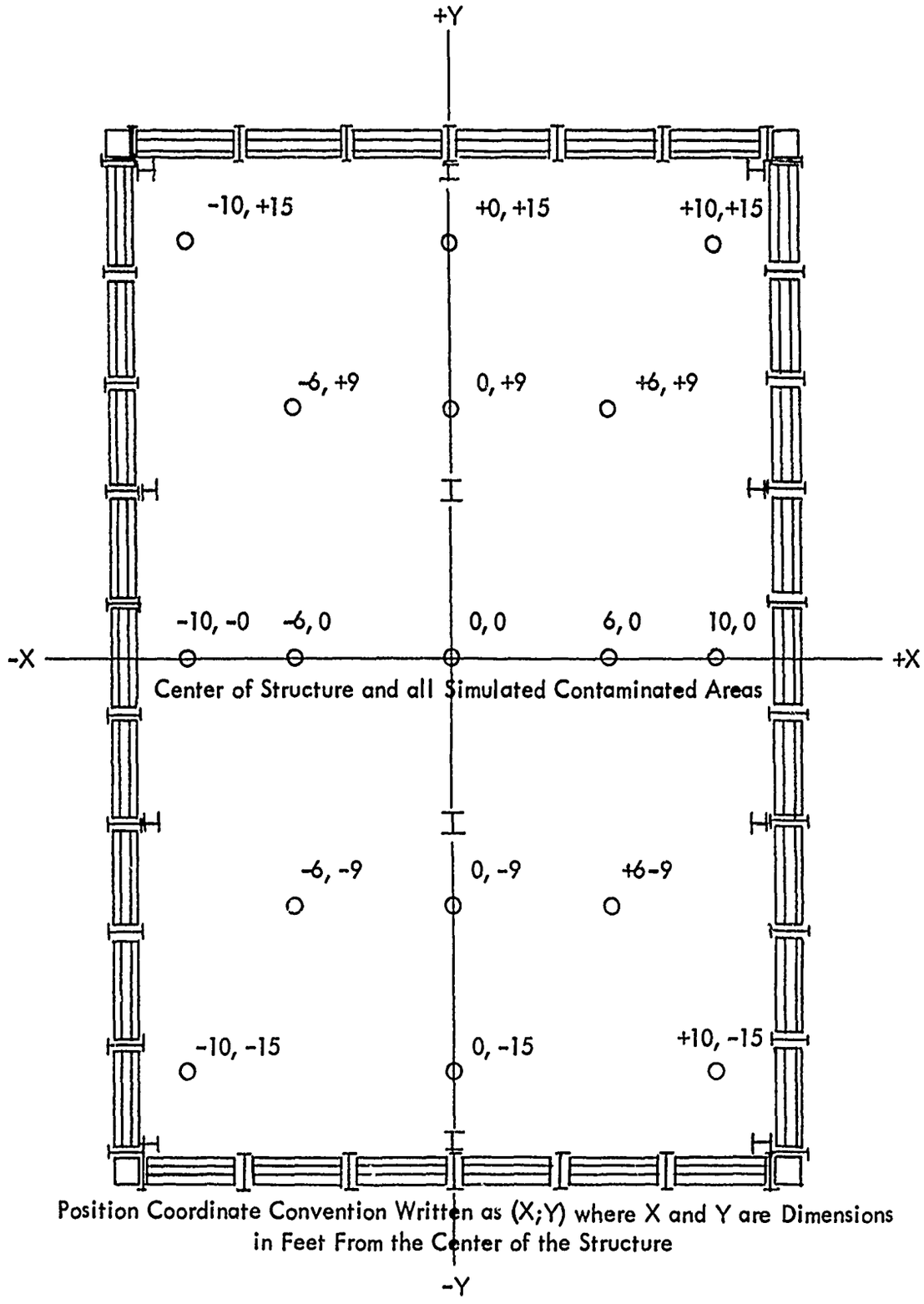

FIG. 3.4 - SKETCH OF COORDINATE CONVENTION IN TEST STRUCTURE

of previously published data[3] of a nearly identical situation, with and without the effect of the supporting beams, indicated however, that this effect, while large, did not invalidate the comparison of experimental results with theoretical ones based on attenuation through concrete alone.

Tables 3.2 through 3.5 present reduction factors measured on the roof centerline (perpendicular to the plane of the roof) as a function of the detector position and the solid angle fraction of the simulated area of contamination (for structures with both 4- and 8-inch floors) for source geometries of a fully contaminated roof (a 36 by 24 foot rectangle) and an 11.5-foot diameter circle. The calculated reduction factors, $L(X)L_a(X, \omega)$ and $L(X)\ L_c\ (X, \omega)$, are also presented in these tables, together with the ratio of the theoretical to experimental reduction factor at each location. These data are also presented graphically in Figures 3.5 and 3.6. It should be noted that the theoretical values of reduction factors were created by summing angular distributions that were computed in infinite media geometry. Thus both functions $L_a\ (X, \omega)$ and $L_c(X, \omega)$ contained radiation backscattered from the atmospheric mass behind the roof (skyshine). The experiments described in this study did not contain this quantity as contamination was simulated only on the roof of the structure, and the majority of the skyshine contribution originates a mean free path ($\sim$450 feet in air) or more away. An estimate of this quantity however, may be made by the following equation using the data of NBS Monograph[2] for Co-60 radiation:

$$D_{sk} = S(d)\ S_a(d, \omega)$$

where

D_{sk} = skyshine dose from an infinite field of Co-60 radiation normalized such that the total dose at a height of 3 feet is equal to 1.0 R/hr

d = mass thickness of the ceiling expressed in terms of equivalent thickness of air=13.3 times thickness in psf

ω = solid angle fraction through which the detector views the skyshine (centered about a perpendicular to the plane of contamination and looking away from it)

TABLE 3.1

EXPECTED STANDARD DEVIATION OF ERROR
(Percent)

Concrete Thickness Between Source and Detector		Error in Dose Rate	Error in Reduction Factor
Inches	PSF	Percent	Percent
0	0	5.0	6.2
4	48.6	5.3	6.5
8	97.2	6.1	7.1
12	145.8	7.2	8.1
16	194.4	8.6	9.4
24	243.0	11.6	12.2

3.6 ANALYSIS OF EXPERIMENTAL RESULTS

In this section the results of the experiments described above are presented, together with calculated values of reduction factors obtained by a method similar to the OCD PM-100-1[1] using attenuation functions representing the mass concentrated at the source and evenly distributed between source and detector. The theoretical values of these functions $L(X)\ L_a(X, \omega)$ and $L(X)\ L_c(X, \omega)$ respectively, were taken from NBS Monograph 42[2] since it was desired to compare the experiments with a Co-60 source rather than a fallout source of contamination. This was done so that conclusions drawn were not affected by the choice of energy spectrum and hence were applicable to fallout as well. The data were also analyzed and compared in the light of previous full-scale experimental work performed at the Protective Structures Development Center. The theoretical function, $L(X)\ L_b(X, \omega)$ is not investigated in this report since the physical arrangement used in the experiment was not representative of this source-barrier-detector configuration.

3.6.1 Comparison of Experimental Data with Theory

An "exact" comparison of the experimental results with theory was not possible because of the effect on the gamma dose rate within the building of the non uniform mass distribution caused by the steel support beams (not "handleable" in the theoretical model) in the test structure. Analysis

TABLE 3.2

Reduction Factors From a Rectangular Roof Source
(48.6 psf Roof and Floors; 24' by 36' Source; Centerline Position)

Detector to Source Plane (ft)	Solid Angle Fraction	Reduction Factors			Ratio Theory to Exp.	
		Exp.	L(X) La (X, ω)	L(X) Lc (X, ω)	L(X) La (X, ω) / Exp.	L(X) Lc (X, ω) / Exp.
★★★★★★★★★★★★★★★★★★★★★★ CONTAMINATION ★★★★★★★★★★★★★★★★★★★★★★						
////////////////// Four Inches Concrete //////////////////						
1.3	0.910	3.53×10^{-2}	5.90×10^{-2}	7.10×10^{-2}	1.67	2.01
2.0	0.870	4.50×10^{-2}	5.80×10^{-2}	7.10×10^{-2}	1.29	1.58
3.0	0.810	4.61×10^{-2}	5.65×10^{-2}	7.00×10^{-2}	1.23	1.52
4.0	0.750	4.57×10^{-2}	5.50×10^{-2}	6.80×10^{-2}	1.20	1.49
5.0	0.700	4.59×10^{-2}	5.40×10^{-2}	6.50×10^{-2}	1.18	1.42
6.0	0.643	4.33×10^{-2}	5.15×10^{-2}	6.20×10^{-2}	1.19	1.43
7.0	0.595	4.09×10^{-2}	4.90×10^{-2}	5.90×10^{-2}	1.20	1.44
8.0	0.550	3.97×10^{-2}	4.65×10^{-2}	5.60×10^{-2}	1.17	1.41
9.0	0.510	3.77×10^{-2}	4.45×10^{-2}	5.25×10^{-2}	1.18	1.39
10.0	0.470	3.60×10^{-2}	4.20×10^{-2}	5.00×10^{-2}	1.17	1.39
11.0	0.433	3.45×10^{-2}	4.00×10^{-2}	4.60×10^{-2}	1.16	1.33
		Standard deviation and mean value of ratios			1.185±.024	1.424±.052
////////////////// Four Inches Concrete //////////////////						
14.0	0.345	6.85×10^{-3}	9.50×10^{-3}	1.25×10^{-2}	1.39	1.82
15.0	0.320	7.11×10^{-3}	8.90×10^{-3}	1.20×10^{-2}	1.25	1.69
16.0	0.298	7.00×10^{-3}	8.40×10^{-3}	1.12×10^{-2}	1.20	1.60
17.0	0.277	6.75×10^{-3}	7.90×10^{-3}	1.06×10^{-2}	1.17	1.57
18.0	0.260	6.40×10^{-3}	7.50×10^{-3}	1.02×10^{-3}	1.17	1.59
19.0	0.241	5.97×10^{-3}	7.00×10^{-3}	9.70×10^{-3}	1.17	1.62
20.0	0.227	5.73×10^{-3}	6.60×10^{-3}	9.20×10^{-3}	1.15	1.61
21.0	0.211	5.37×10^{-3}	6.30×10^{-3}	8.70×10^{-3}	1.17	1.62
22.0	0.200	5.13×10^{-3}	6.00×10^{-3}	8.40×10^{-3}	1.17	1.64
23.0	0.186	4.89×10^{-3}	5.70×10^{-3}	7.90×10^{-3}	1.17	1.62
		Standard deviation and mean value of ratios			1.170±.010	1.612±.030
////////////////// Four Inches Concrete //////////////////						
25.3	0.162	7.84×10^{-4}	1.61×10^{-3}	2.50×10^{-3}	2.05	3.19
26.3	0.152	9.53×10^{-4}	1.52×10^{-3}	2.39×10^{-3}	1.59	2.51
27.3	0.143	1.00×10^{-3}	1.44×10^{-3}	2.25×10^{-3}	1.44	2.25
28.3	0.135	1.01×10^{-4}	1.39×10^{-3}	2.14×10^{-3}	1.38	2.12
29.3	0.128	9.76×10^{-4}	1.31×10^{-3}	2.04×10^{-3}	1.34	2.09
30.3	0.121	9.37×10^{-4}	1.28×10^{-3}	2.00×10^{-3}	1.37	2.13
31.3	0.115	8.90×10^{-4}	1.22×10^{-3}	1.90×10^{-3}	1.37	2.13
32.3	0.109	8.66×10^{-4}	1.15×10^{-3}	1.80×10^{-3}	1.33	2.08
33.3	0.104	8.41×10^{-4}	1.11×10^{-3}	1.75×10^{-3}	1.32	2.08
34.3	0.100	8.79×10^{-4}	1.08×10^{-3}	1.70×10^{-3}	1.23	1.93
35.3	0.097	7.74×10^{-4}	1.03×10^{-3}	1.62×10^{-3}	1.33	2.09
		Standard deviation and mean value of ratios			1.348±.050	2.105±.060

TABLE 3.3

Reduction Factors From a Circular Roof Source
(48.6 psf Roof and Floors; 11.5' dia. source; Centerline Position)

Detector to Source Plane (ft)	Solid Angle Fraction	Reduction Factors			Ratio Theory to Exp.	
		Exp.	L(X) La (X, ω)	L(X) Lc (X, ω)	L(X) La (X, μ) / Exp.	L(X) Lc (X, ω) / Exp.
********** CONTAMINATION **********						
////////// Four Inches Concrete //////////						
1.3	0.770	2.78×10^{-2}	5.60×10^{-2}	6.80×10^{-2}	2.01	2.45
2.0	0.660	3.59×10^{-2}	5.20×10^{-2}	6.30×10^{-2}	1.45	1.75
3.0	0.530	3.41×10^{-2}	4.60×10^{-2}	5.40×10^{-2}	1.35	1.58
4.0	0.420	3.14×10^{-2}	3.90×10^{-2}	4.50×10^{-2}	1.24	1.43
5.0	0.345	2.44×10^{-2}	3.35×10^{-2}	3.80×10^{-2}	1.37	1.56
6.0	0.280	2.06×10^{-2}	2.80×10^{-2}	3.10×10^{-2}	1.36	1.50
7.0	0.232	1.70×10^{-2}	2.40×10^{-2}	2.54×10^{-2}	1.41	1.49
8.0	0.190	1.42×10^{-2}	2.00×10^{-2}	2.10×10^{-2}	1.41	1.48
9.0	0.160	1.25×10^{-2}	1.70×10^{-2}	1.71×10^{-2}	1.36	1.37
10.0	0.135	1.06×10^{-2}	1.42×10^{-2}	1.45×10^{-2}	1.34	1.37
11.0	0.115	9.57×10^{-3}	1.20×10^{-2}	1.22×10^{-2}	1.25	1.27
		Standard deviation and mean value of ratios			1.360±.060	1.470±.135
////////// Four Inches Concrete //////////						
14.0	0.075	1.56×10^{-3}	2.90×10^{-3}	3.60×10^{-3}	1.86	2.31
15.0	0.066	1.65×10^{-3}	2.30×10^{-3}	3.10×10^{-3}	1.39	1.88
16.0	0.059	1.52×10^{-3}	2.03×10^{-3}	2.75×10^{-3}	1.34	1.81
17.0	0.053	1.43×10^{-3}	1.83×10^{-3}	2.49×10^{-3}	1.28	1.74
18.0	0.0475	1.26×10^{-3}	1.64×10^{-3}	2.20×10^{-3}	1.30	1.75
19.0	0.043	1.19×10^{-3}	1.50×10^{-3}	2.00×10^{-3}	1.26	1.68
20.0	0.039	1.10×10^{-3}	1.38×10^{-3}	1.81×10^{-3}	1.25	1.65
21.0	0.0354	1.03×10^{-3}	1.24×10^{-3}	1.67×10^{-3}	1.20	1.62
22.0	0.0324	9.66×10^{-4}	1.14×10^{-3}	1.53×10^{-3}	1.18	1.58
23.0	0.030	9.86×10^{-4}	1.07×10^{-3}	1.41×10^{-3}	1.21	1.59
		Standard deviation and mean value of ratios			1.258±.096	1.685±.130
////////// Four Inches Concrete //////////						
25.3	0.025	1.54×10^{-4}	2.85×10^{-4}	4.55×10^{-4}	1.85	2.95
26.3	0.023	1.68×10^{-4}	2.68×10^{-4}	4.22×10^{-4}	1.60	2.51
27.3	0.021	1.67×10^{-4}	2.50×10^{-4}	3.94×10^{-4}	1.50	2.36
28.3	0.020	1.72×10^{-4}	2.31×10^{-4}	3.62×10^{-4}	1.34	2.10
29.3	0.019	1.56×10^{-4}	2.18×10^{-4}	3.40×10^{-4}	1.40	2.18
30.3	0.018	1.48×10^{-4}	2.04×10^{-4}	3.20×10^{-4}	1.38	2.16
31.3	0.016	1.39×10^{-4}	1.91×10^{-4}	3.00×10^{-4}	1.37	2.16
32.3	0.016	1.33×10^{-4}	1.81×10^{-4}	2.80×10^{-4}	1.36	2.11
33.3	0.015	1.31×10^{-4}	1.71×10^{-4}	2.63×10^{-4}	1.31	2.01
34.3	0.014	1.22×10^{-4}	1.62×10^{-4}	2.50×10^{-4}	1.33	2.05
35.3	0.013	1.17×10^{-4}	1.55×10^{-4}	2.34×10^{-4}	1.32	2.00
		Standard deviation and mean value of ratios			1.368±0.052	2.125±.145

TABLE 3.4

Reduction Factors From a Rectangular Roof Source
(97.2 psf Roof and Floors; 24' by 36' Source; Centerline Position)

Detector to Source Plane (ft)	Solid Angle Fraction (ω)	Reduction Factors			Ratio Theory to Exp.	
		Exp.	L(X) La (X, ω)	L(X) Lc (X, ω)	$\frac{L(X)\ La\ (X,\omega)}{Exp.}$	$\frac{L(X)\ Lc\ (X,\omega)}{Exp.}$
		Third Floor Detectors (Eight Inch Concrete Roof)				
2	0.870	9.70×10^{-3}	1.50×10^{-2}	1.78×10^{-2}	1.55	1.84
3	0.810	1.12×10^{-2}	1.44×10^{-2}	1.76×10^{-2}	1.29	1.57
4	0.750	1.14×10^{-2}	1.41×10^{-2}	1.74×10^{-2}	1.24	1.53
5	0.700	1.14×10^{-2}	1.39×10^{-2}	1.70×10^{-2}	1.22	1.49
6	0.643	1.13×10^{-2}	1.33×10^{-2}	1.68×10^{-2}	1.18	1.49
7	0.595	1.08×10^{-2}	1.29×10^{-2}	1.63×10^{-2}	1.19	1.51
8	0.550	1.06×10^{-2}	1.23×10^{-2}	1.60×10^{-2}	1.16	1.51
9	0.510	1.03×10^{-2}	1.20×10^{-2}	1.58×10^{-2}	1.17	1.53
10	0.470	9.81×10^{-3}	1.14×10^{-2}	1.52×10^{-2}	1.16	1.55
11	0.433	9.78×10^{-3}	1.10×10^{-2}	1.48×10^{-2}	1.12	1.51
		Mean value and standard deviation of ratios			1.182±.063	1.507±.044
		Second Floor Detectors (Eight Inch Concrete Roof and Eight Inch Concrete Floor)				
14	0.345	4.44×10^{-4}	7.30×10^{-4}	1.20×10^{-3}	1.64	2.70
15	0.320	5.09×10^{-4}	7.10×10^{-4}	1.16×10^{-3}	1.39	2.28
16	0.298	5.30×10^{-4}	6.80×10^{-4}	1.12×10^{-3}	1.28	2.11
17	0.277	5.30×10^{-4}	6.50×10^{-4}	1.10×10^{-3}	1.23	2.08
18	0.260	5.13×10^{-4}	6.30×10^{-4}	1.05×10^{-3}	1.23	2.05
19	0.241	4.89×10^{-4}	6.00×10^{-4}	1.00×10^{-3}	1.23	2.04
20	0.227	4.63×10^{-4}	5.70×10^{-4}	9.50×10^{-4}	1.23	2.05
21	0.211	4.42×10^{-4}	5.40×10^{-4}	9.10×10^{-4}	1.22	2.06
22	0.200	4.25×10^{-4}	5.20×10^{-4}	8.80×10^{-4}	1.22	2.07
23	0.186	4.14×10^{-4}	5.00×10^{-4}	8.40×10^{-4}	1.21	2.03
		Mean value and standard deviation of ratios			1.225±.013	2.066±.034

TABLE 3.5

Reduction Factors From a Circular Roof Source
(97.2 psf Roof and Floors; 11.5' dia. source; Centerline Position)

Detector to Source Plane (ft)	Solid Angle Fraction (ω)	Reduction Factors			Ratio Theory to Exp.	
		Exp.	L(X) La (X, ω)	L(X) Lc (X, ω)	$\frac{L(X)\ La\ (X,\omega)}{Exp.}$	$\frac{L(X)\ Lc\ (X,\omega)}{Exp.}$
		Third Floor Detectors (Eight Inch Concrete Roof)				
2	0.660	9.05×10^{-3}	1.40×10^{-2}	1.70×10^{-2}	1.55	1.88
3	0.530	9.16×10^{-3}	1.22×10^{-2}	1.60×10^{-2}	1.33	1.75
4	0.420	8.71×10^{-3}	1.08×10^{-2}	1.43×10^{-2}	1.24	1.64
5	0.345	7.59×10^{-3}	9.50×10^{-3}	1.26×10^{-2}	1.25	1.66
6	0.280	6.38×10^{-3}	8.00×10^{-3}	1.09×10^{-2}	1.25	1.71
7	0.232	5.47×10^{-3}	6.80×10^{-3}	9.50×10^{-3}	1.24	1.74
8	0.190	4.74×10^{-3}	5.80×10^{-3}	8.00×10^{-3}	1.22	1.69
9	0.160	4.09×10^{-3}	5.15×10^{-3}	7.00×10^{-3}	1.26	1.71
10	0.135	3.58×10^{-3}	4.40×10^{-3}	6.10×10^{-3}	1.23	1.70
11	0.115	3.15×10^{-3}	3.90×10^{-3}	5.50×10^{-3}	1.24	1.75
		Mean value and standard deviation of ratios			1.242± .016	1.702± .040
		Second Floor Detectors (Eight Inch Concrete Roof and Eight Inch Concrete Floor)				
14	0.075	1.75×10^{-4}	2.43×10^{-4}	4.20×10^{-4}	1.39	2.40
15	0.066	1.80×10^{-4}	2.20×10^{-4}	3.80×10^{-4}	1.22	2.11
16	0.059	1.79×10^{-4}	1.97×10^{-4}	3.41×10^{-4}	1.10	1.91
17	0.053	1.64×10^{-4}	1.80×10^{-4}	3.10×10^{-4}	1.10	1.89
18	0.048	1.45×10^{-4}	1.61×10^{-4}	2.30×10^{-4}	1.11	1.93
19	0.043	1.35×10^{-4}	1.48×10^{-4}	2.50×10^{-4}	1.10	1.85
20	0.039	1.21×10^{-4}	1.36×10^{-4}	2.30×10^{-4}	1.12	1.90
21	0.035	1.11×10^{-4}	1.23×10^{-4}	2.10×10^{-4}	1.11	1.89
22	0.032	1.05×10^{-4}	1.13×10^{-4}	1.93×10^{-4}	1.08	1.84
23	0.030	9.44×10^{-5}	1.06×10^{-4}	1.80×10^{-4}	1.12	1.91
		Mean value and standard deviation of ratios			1.105± .017	1.895± .045

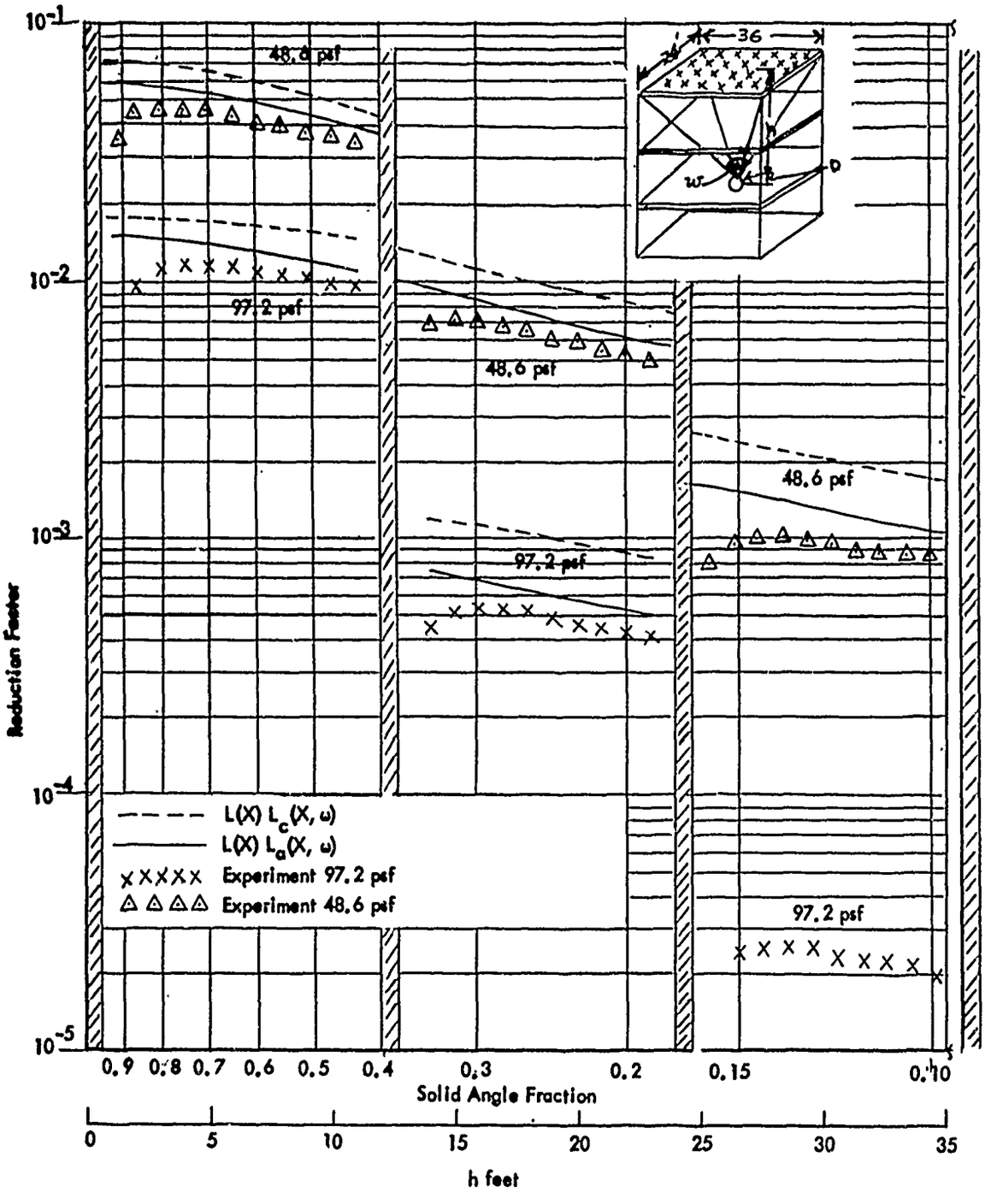

FIG. 3.5 - Calculated and Experimental Reduction Factors for 48.6 psf and 97.2 psf Mass Thickness Floors. Full Roof Contamination

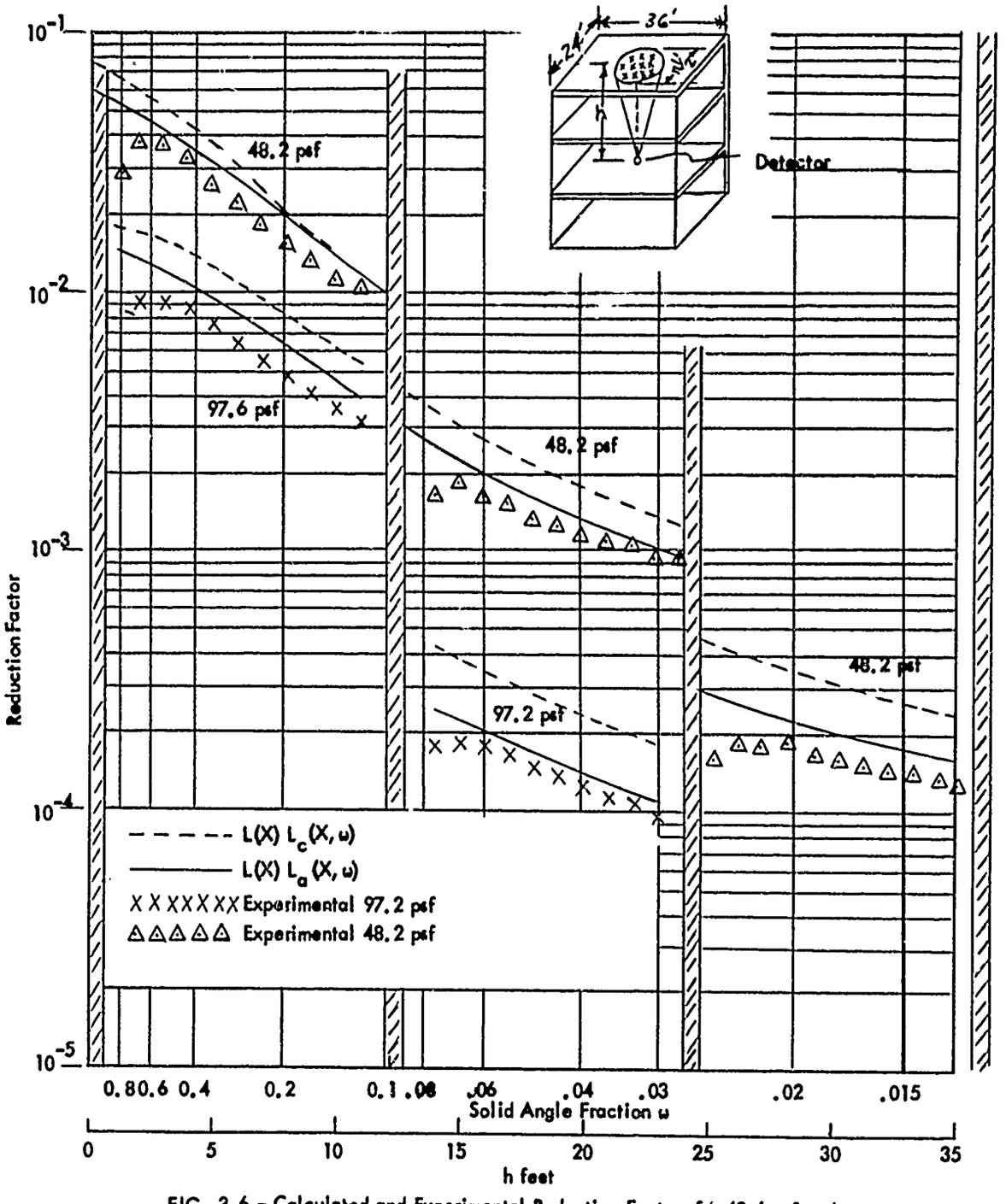

FIG. 3.6 - Calculated and Experimental Reduction Factors for 48.6 psf and 96.2 psf Floors, 11.5 ft Diameter Circular Area of Contamination on Roof

$S_a(d, \omega)$ = anguiar distribution of skyshine dose (note Sa $(d, \omega) = 1$ at $\omega=1$)

If D_{sk} is evaluated, it is found to be very small in all cases covered in this study (thickness $\geq$ 48.6 psf). The maximum effect expressed in terms of equivalent massthickness of the roof was of the order 1 psf for the case of the 48.6 psf roof. Thus, the lack of adequate simulation of sky-shine in the experiment caused the roof to appear to be a maximum of a-bout 1 psf more in thickness for the thin roof (48.6 psf total thickness) and the apparent increase in thickness was negligible in all other cases.

Tables 3.2 through 3.5 indicate that either of the theoretical functions always yields a conservative value (calculated reduction factor greater numerically than measured) of the roof reduction factor. The attenuation afforded by the support beams of the structure could, however, account for at least part of this difference. It is important to determine if the theoretical value of $L(X)\ L_c\ (X, \omega)$ or $L(X)\ L_a\ (X, \omega)$ would or would not underestimate the roof reduction factors within the structure if the support beams had been absent.

The effectveness of any given amount of mass in attenuating radiation emanating from an isotropic plane source is decreased if the mass is lumped in discrete masses rather than spread uniformly to attenuate all radiation. This is because radiation is attenuated exponentially, while mass is distributed arithmetically. For example, the mass required to reduce the dose rate eminating from a uniformly contaminated infinite place of 1.25 Mev radiation by a factor of ten is 41 PSF. If this same total mass per unit area were lumped into areas of zero PSF and 410 PSF thickness, the percentage of the contaminated plane that was shielded by 410 PSF would by only 10%, thus the total dose rate measured above the plane with lumped masses would by slightly more than 90% of that from the unshielded source plane or nine times greater than if the same amount of mass had been uniformly distributed over the source plane.

Thus a conservative estimate of the worth of the steel beams could be gained by "smearing" the steel over the entire area of the floor. In other words, the total amount of steel per floor is calculated and the smeared thickness of an equal weight steel plate is obtained. This must then by multiplied by 0.931 to correct for the deficiency of electrons in iron per unit mass compared with concrete[2]. This smeared thickness has been calculated to be approximately 9.6 psf per floor.

Table 3.6 summarizes the data of Tables 3.2 through 3.5 in the form of mean values and standard deviations of the ratio of a theoretically calculated dose to that measured experimentally. An effective floor thickness may thus be determined for each method (that required to reduce the mean value of the ratio of calculated-to-measured-dose rate to 1.0) of computation. Comparable cases are presented in Table 3.6 together with the difference between this "effective" floor thickness and the actual thickness of concrete. Inspection of these differences indicates that even if the support beams were as effective as if their mass were smeared over the entire floor areas, the function $L(X)\, L_c(X, \omega)$ would serve as a maximum upper limit to the roof reduction factors. However, since the effect of inhomogeneous mass distribution must be less than if the steel were smeared, $L(X)L_a\ (X, \omega)$, in all probability, represents a realistic value.

Previous work[3] in idealized geometry with the mass concentrated adjacent to the source (and with a scattering mass behind the source to reproduce the skyshine effect) indicated that the best agreement between theory and experiment could be obtained in the case of a 48.6 psf (4-inch concrete) shield if theoretical calculations were based on 55 psf; similarly for a 97.2 psf shield calculation for 100 psf and for a 145.8 chield calculation for 146 psf. If these higher values are taken as the effective thickness of the concrete shield, an estimate of the steel effectineness may be made. This effect of the steel is presented in the right hand column of Table 3.6. Note that in the previous work the mass was concentrated only at the source, thus this is the only situation that may be compared directly. Since the difference between experimentally measured dose rates and those theoretically calculated (expressed as equivalent mass thickness in Table 3.6) is greater than the effect of the support beams, with the experimentally measured dose always lower than that calculated, both of the methods of calculation ($L(X)L_a(X, \omega)$ and $L(X)\, L_c\ (X, \omega)$ yield conservative results.

The function $L(X)\, L_a\ (X, \omega)$, however, seems more representative of the actual reduction factor than that presently used[1] $L(X)\, L_c\ (X, \omega)$. Since the use of $L(X)\, L_a\ (X, \omega)$ may increase predicted protection factors significantly in some cases, further experimental and theoretical work on inhomogenous roof slabs is warranted.

The data of this experiment may also be used to illustrate the difference represented by the theoretical functions $L(X)\, L_c\ (X, \omega)$ and $L(X)L_a(X, \omega)$. These functions $L(X)\, L_c\ (X, \omega)$ and $L(X)\, L_a\ (X, \omega)$ represent, respectively, the case in which the barrier is uniformly distributed between source and de-

tector and the case in which the barrier is concentrated near the source. The former case predicts a higher roof contribution than the latter over the range of the investigation where X varied from 48.6 psf to 291.6 psf. Experimental verification of this effect is presented for 8 inches of concrete in Figure 3.7 where measured values of the roof reduction factor for the case of two 4-inch floors separated by 12 feet of open space and the case of an 8-inch solid roof adjacent to the source in an open structure of simple box geometry are presented. The difference between these two sets of experimental data is observed to be similar but not so great as theory would predict. Thus, here again there exists an indication that the $L(X)\, L_c\, (X, \omega)$ function may be overly conservative in predicting the effect of discrete floor masses.

3.6.2 Off-center positions

In the case of the entire roof of the structure being covered with simulated contamination, detectors were placed along both the vertical centerline and at various off-center locations. Figure 3.4 shows the off-center dosimeter locations in the test structure. The data from these experiments expressed as roof reduction factors, for the off-center locations are presented in Table 3.7 for both structures (4- and 8-inch floor thicknesses) tested. A typical comparison of experiment with theory is shown in Figure 3.8. Where the theoretical values were calculated by the "fictitious building" method described in Append[illegible] No new information is evidenced in this comparison; however, it [illegible]ing to note that experiment and theory compare in the same fashi[illegible]f-center positions as for those on the vertical centerline. This observation was previously made in Ref. 3 in which only the case of the mass adjacent to the source (i.e., single-story structures) was investigated. The conclusion previously made ——that the "fictitious building" method of calculating off-center roof reduction factors is at least as valid as the method used for centerline positions —— remains valid.

Diagonal traverses of the roof reduction factors for the full roof source for various heights in each structure are also presented in Figure 3.8. The experimental points are shown together with the calculated values. Here again the same conclusion as above can be drawn from these plots as to the accuracy of the "fictitious building" method.

TABLE 3.6

Summary of Centerline Detector Data

Number of Slabs Between Source and Detector	Total Concrete Thickness (inches)	Mean Value and Std. Deviation Theory Divided by Experiment		Psf Required in Theory for Agreement		Difference psf		Effect of Steel Directly Comparable Cases Only psf
		$L(X)La(X,\omega)$ /Exp.	$L(X)Lc(X,\omega)$/ Exp.	$L(X)La(X,\omega)$	$L(X)Lc(X,\omega)$	$L(X)La(X,\omega)$	$L(X)Lc(X,\omega)$	
4 inch Floors 24 x 36 ft. Roof Contamination								
1	4	1.185± .024	1.424± .052	56	64	7	15	1
2	8	1.70± .010	1.612± .030	105	121	7	23	-
3	12	1.348± .050	2.105± .060	159	180	12	33	-
4 inch Floors 11.5 ft. dia Roof Contamination								
1	4	1.360± .060	1.470± .135	61	67	12	18	6
2	8	1.258± .096	1.685± .130	112	128	14	30	-
3	12	1.368± .052	2.125± .145	160	180	13	33	-
8 inch Floors 24 x 36 ft. Roof Contamination								
1	8	1.182± .063	1.507± .044	105	115	7	17	5
2	16	1.225± .013	2.066± .034	204	223	8	27	-
8 inch Floors 11.5 ft. dia Roof Contamination								
1	8	1.242± .16	1.702± .040	107	121	9	23	7
2	16	1.105± .017	1.895± .045	200	224	4	28	-

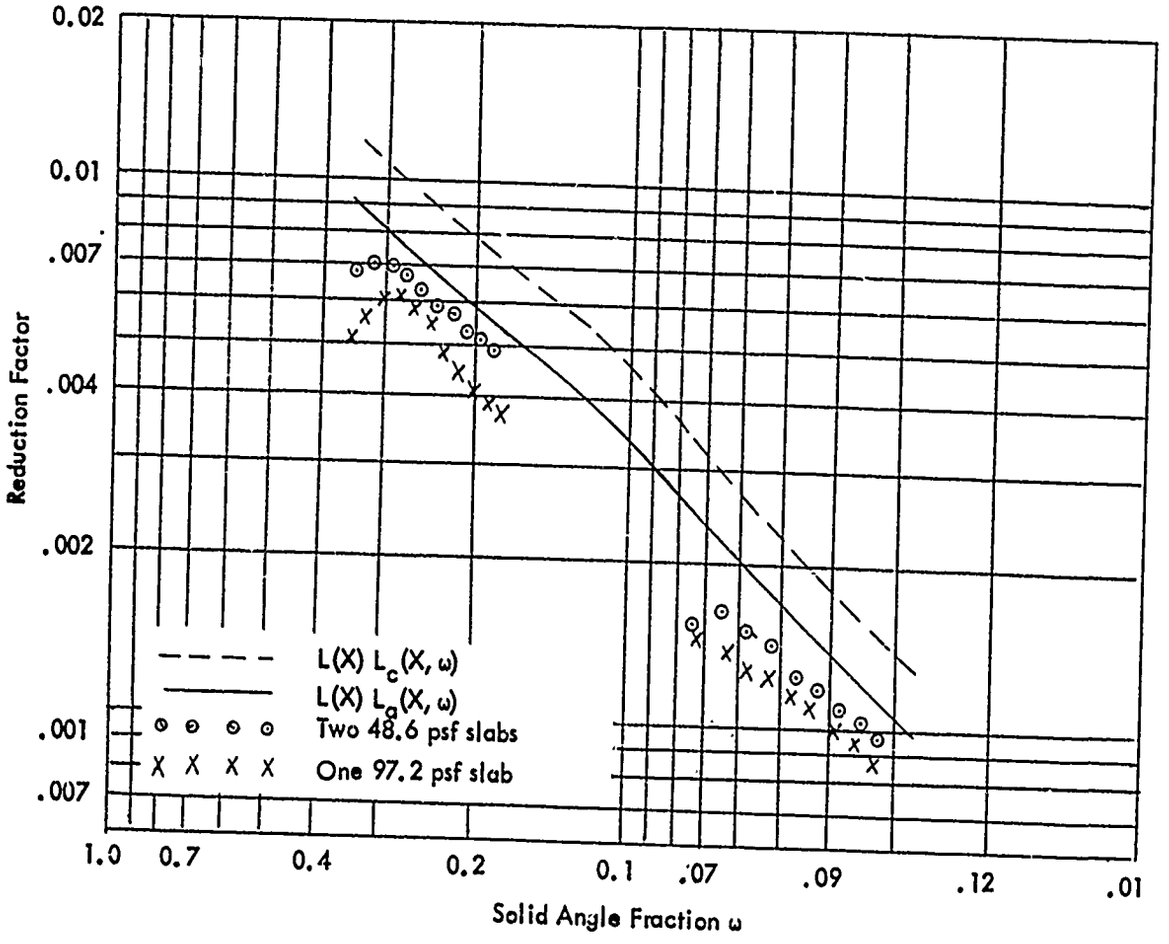

FIG. 3.7 – Comparison of Theory with Experiment for 97.2 psf Floor Thickness Between Source and Detector for Both a Single and Divided Slab (Two 48.6 psf Slabs Separated by a Distance of 12 ft)

TABLE 3.7

Typical Roof Reduction Factors Off Center Positions
(24 x 36 ft. Rectangular Source)

Distance to Source (ft)	Number of Barriers Between Source and Detector	X, Y Positions (see Fig. 3.4)					
		10, 15	6, 9	0, 15	0, 9	6, 0	10, 0
4 Inch Roof and Floors							
3.0	1	3.62×10^{-2}	4.55×10^{-2}	4.29×10^{-2}	4.57×10^{-2}	4.66×10^{-2}	4.05×10^{-2}
6.0	1	2.41×10^{-2}	3.84×10^{-2}	3.34×10^{-2}	4.07×10^{-2}	4.00×10^{-2}	3.08×10^{-2}
9.0	1	1.97×10^{-2}	3.23×10^{-2}	2.74×10^{-2}	3.51×10^{-2}	3.45×10^{-2}	2.69×10^{-2}
15.0	2	3.70×10^{-3}	6.10×10^{-3}	5.00×10^{-3}	6.00×10^{-3}	7.00×10^{-3}	5.40×10^{-3}
18.0	2	3.10×10^{-3}	5.10×10^{-3}	4.40×10^{-3}	5.30×10^{-3}	5.90×10^{-3}	4.50×10^{-3}
21.0	2	2.90×10^{-3}	4.30×10^{-3}	3.70×10^{-3}	4.70×10^{-3}	4.80×10^{-3}	3.90×10^{-3}
26.3	3	6.70×10^{-4}	9.80×10^{-4}	7.60×10^{-4}	———	1.10×10^{-3}	9.40×10^{-4}
29.3	3	5.40×10^{-4}	8.00×10^{-4}	7.30×10^{-4}	8.50×10^{-4}	9.20×10^{-4}	7.60×10^{-4}
32.3	3	4.90×10^{-4}	6.90×10^{-4}	6.60×10^{-4}	7.50×10^{-4}	8.00×10^{-4}	6.80×10^{-4}
8 Inch Roof and Floors							
3.0	1	1.01×10^{-2}	$.17 \times 10^{-2}$	1.09×10^{-2}	1.09×10^{-2}	1.18×10^{-2}	1.08×10^{-2}
6.0	1	6.80×10^{-3}	9.90×10^{-3}	8.70×10^{-3}	1.02×10^{-2}	1.04×10^{-2}	8.40×10^{-3}
9.0	1	5.30×10^{-3}	8.60×10^{-3}	7.50×10^{-3}	9.10×10^{-3}	9.00×10^{-3}	7.30×10^{-3}
15.0	2	3.00×10^{-4}	5.10×10^{-4}	4.00×10^{-4}	5.00×10^{-4}	5.30×10^{-3}	4.00×10^{-4}
18.0	2	2.20×10^{-4}	4.20×10^{-4}	3.50×10^{-4}	4.50×10^{-4}	4.60×10^{-3}	8.40×10^{-4}
21.0	2	2.10×10^{-4}	3.40×10^{-4}	3.20×10^{-4}	3.80×10^{-4}	3.90×10^{-3}	3.10×10^{-4}

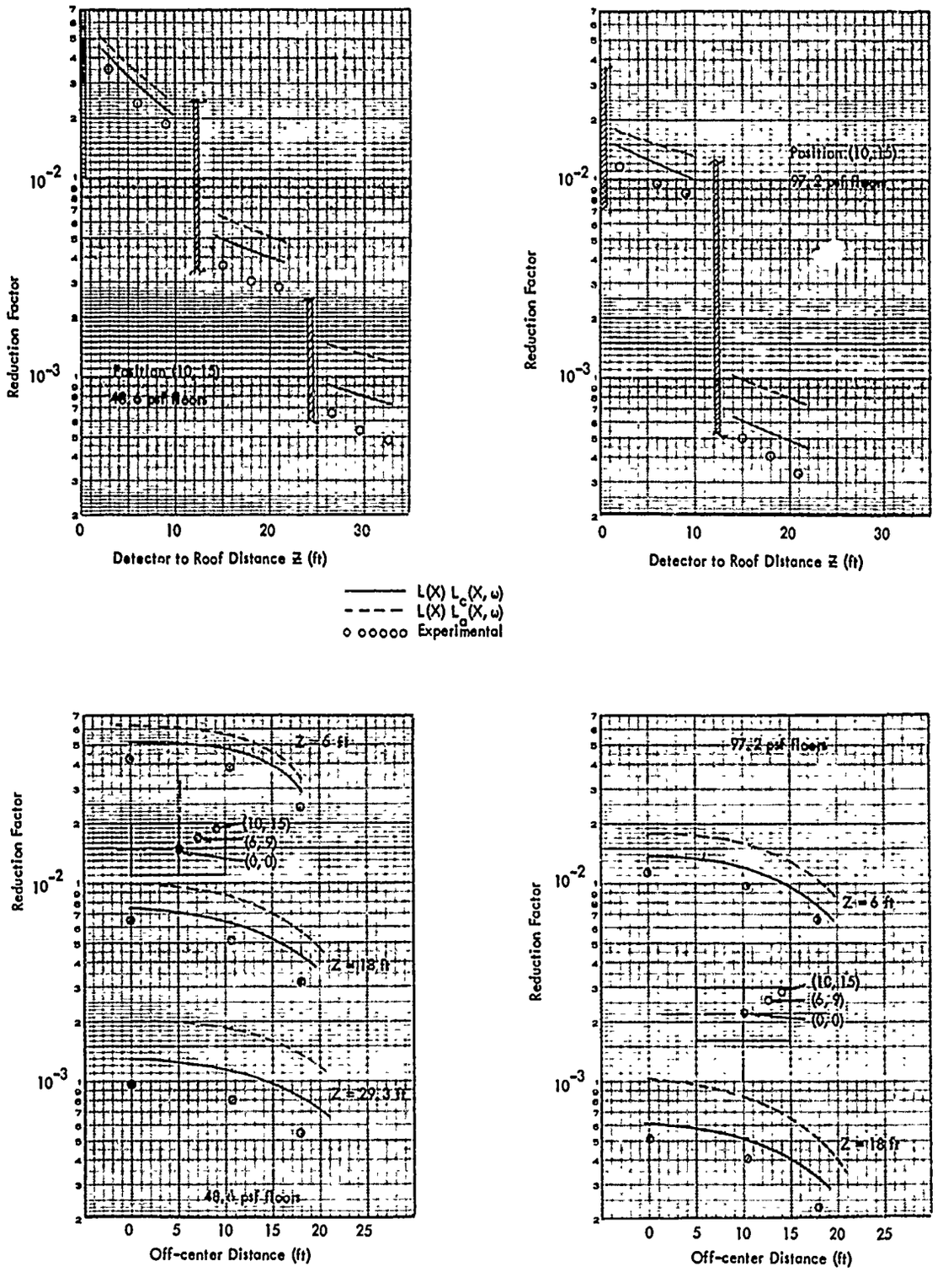

FIG. 3.8 – Comparison of Calculated and Experimentally Measured Roof Reduction Factors Off-Center Positions

CHAPTER 4

CONCLUSIONS AND RECOMMENDATIONS

The purpose of this study was to determine what, if any, significant differences exist in the dose rate from roof-based sources of contamination when the attenuating mass was distributed in finite layers between source and detector rather than concentrated at the source and to compare the dose rates determined with those predicted theoretically. The interpretation of the results obtained is, unfortunately, somewhat clouded by the seemingly minor inhomogeneity of the ceiling slabs and steel supports. This disparity, caused by the support structure was of the same order of magnitude as the effect that was measured. Conclusions as to the validity of currently used theoretical estimates, however, were made by interpreting the results obtained in this study in the light of previously published work.[3]

4.1 CONCLUSIONS

The following conclusions resulted from this study.

1. The experimentally measured roof reduction factors illustrate the same dependence on the solid angle of the contaminated areas of those computed with either function $L(X)L_c(X, \omega)$ or $L(X)\ L_a(X, \omega)$. Measured values were always significantly lower than the ones predicted. When the effect of the floor support beams was neglected, measured values were as much as 25 and 50 percent lower, respectively, than those computed using $L(X)\ L_a(X, \omega)$ and $L(X)\ L_c(X, \omega)$.

2. The current use of the function $L(X)\ L_c(X, \omega)$ to represent the roof reduction factor seems overly conservative. The function $L(X)\ L_a(X, \omega)$ presents a conservative estimate of the dose rates measured.

3. Off-center roof reduction factors calculated by the "fictitious building" method portray the same relative agreement with experiment as do the centerline. This indicates that the off-center reduction factor calculations are as valid as those on the structure centerline.

4.2 RECOMMENDATIONS

The following recommendations are offered as a result of this study.

1. A series of experiments should be undertaken upon roofs of controlled non-uniform thickness to ascertain the best method of calculating the effect of the inhomogeneous distribution of mass in a structure roof since it has been shown to produce fairly major discrepancies in calculated reduction factors.

2. Further measurements should be made of the attenuation afforded by roof and ceiling slabs for idealized geometry in the absence of mass discontinuities.

3. Unless further experiments indicate differently, it is tentatively recommended that the function $L(X)\ L_a(X, \omega)$ rather than $L(X)\ L_c(X, \omega)$ be used to represent a more realistic estimate of the dose attributed to contamination existing on the roof of a structure.

REFERENCES

1. Design and Review of Structures for Protection from Fallout Gamma Radiation OCD PM-100-1 (February 1965).

2. L. V. Spencer, Structure Shielding against Fallout Radiation from Nuclear Weapons, NBS Monograph 42 (June 1962).

3. C. H. McDonnell, J. Velletri, An Experimental Evaluation of Roof Reduction Factors, PSDC-TR-16 (May 1966).

4. C. E. Eisenhauer, An Engineering Method for Calculating Protection Afforded by Structures against Fallout Radiation, OCM PM 100-1, Supplement No. 1 (June 1964).

5. D. J. Raso and S. Woolf, The Dose Resulting from a 1.25 MEV Plane Source Behind Various Arrangement of Iron Barriers, Tech/Ops Corp., TOB-64-49 (June 1964).

6. E. T. Clarke, J. F. Batter, and A. L. Kaplan, Measurement of Attenuation in Existing Structure of Radiation from Simulated Fallout, Tech/OPS Corp. TOB 59-4 (April 1959).

7. E. Titus, Penetration in Concrete of Gamma Radiation from Fallout, NBS Report 6143 (September 1958).

8. J. F. Batter, A. L. Kaplan, and E. T. Clarke, An Experimental Evaluation of the Radiation Protection Afforded by a Large Modern Concrete Office Building, CEX-59.1 (January 1960).

9. M. A. Schmoke and R. E. Rexroad, Attenuation of Simulated Fallout Radiation by the Roof of a Concrete Blockhouse, NDL-TR-6 (August 1961).

10. C. H. McDonnell et al, Description, Experimental Calibration and and Analysis of the Radiation Test Facility at the Protective Structures Development Center, PSDC-TR-14 (September 1964).

APPENDIX A

OFF-CENTER POSITIONS

Off-center reduction factors resulting from roof sources can be calculated using the "fictitious building" method. This method consists of dividing the roof of the structure being considered into two or more imaginary roofs that are symmetrical about the point in question, and hence calculable. It is then assumed that the average of the imaginary roof reduction factors results in the reduction factor of the off-center point considered.

As an example of this procedure, consider a point located at position (6, 9) (x, y coordinates from center of structure) below a rectangular 24- by 36-foot roof of 145.8 psf thickness. The roof area must be divided into four rectangles, each of which is symmetrical about the point of interest. Each of these rectangles, labelled Fictitious Buildings A, B, C, and D in Fig. A-1, represents four times the dose that would be received by a detector from the upper left, upper right, lower left, and lower right quadrants, respectively, if the coordinate axis were centered upon the point of interest. The calculation of the dose from each of these centered rectangles then proceeds in the manner prescribed by the OCD PM 100-1 and is presented below:

Building	Z	W	L	$e=\frac{W}{L}$	$n=\frac{2Z}{L}$	ω	$L(X)L_a(X, \omega)$
A	9	12	18	0.67	1.0	0.27	0.0024
B	9	18	36	0.50	0.50	0.47	0.0031
C	9	12	54	0.22	0.33	0.35	0.0028
D	9	36	54	0.67	0.33	0.65	0.0038

The total of the reduction factor column $(L(X)L_a(X, \omega)$ divided by 4 thus represents the expected reduction factor below the point 6, 9. Thus:

$$\text{Total } L(X)L_a(X, \omega) = 0.0121$$

$$\text{Reduction factor} = \frac{0.0121}{4} = 0.0030$$

[1] Design and Review of Structures for Protection from Fallout Gamma Radiation, OCD PM-100-1 (February 1965)

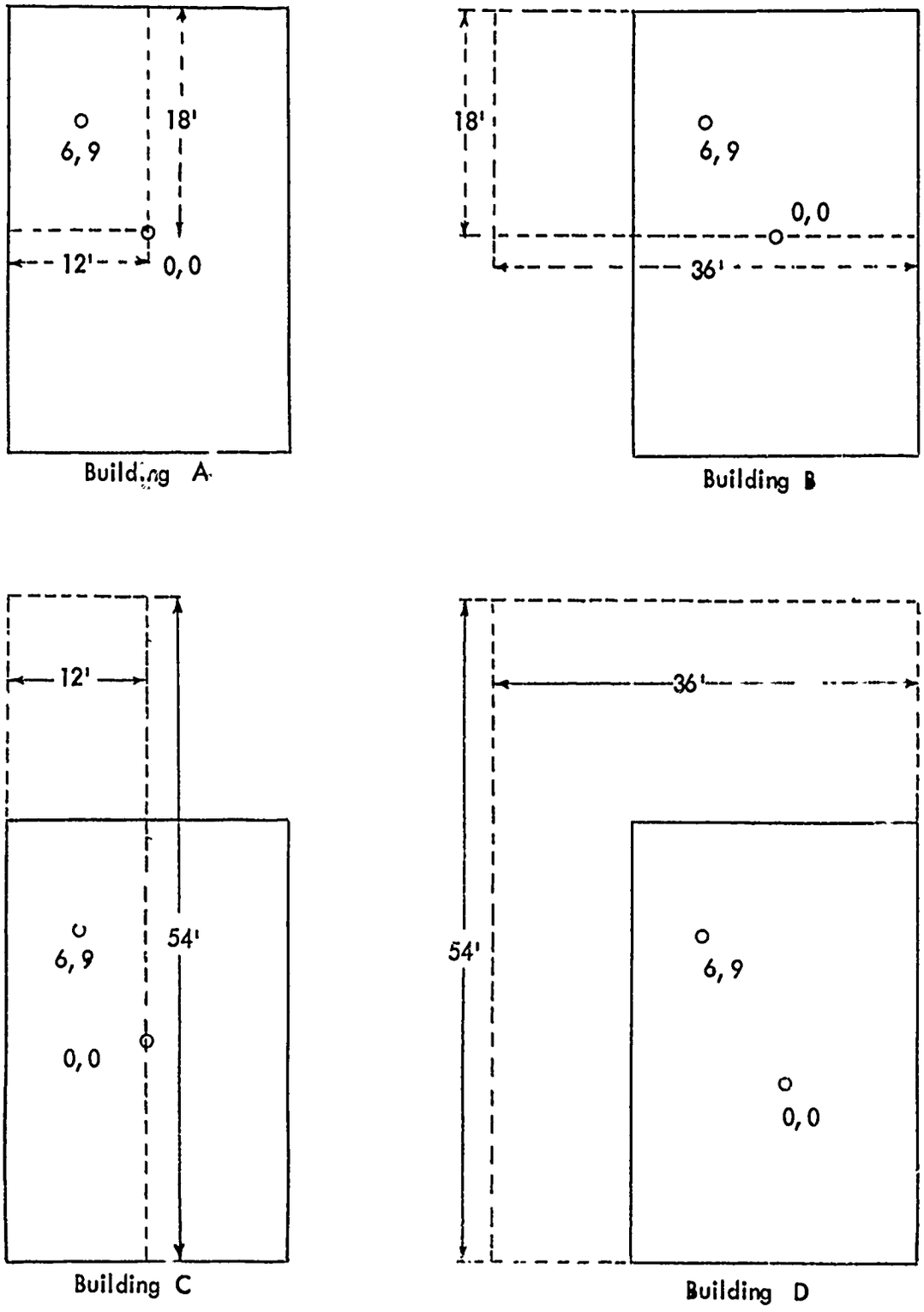

FICTITIOUS BUILDINGS FOR POSITION 6, 9

Figure A-1

BLANK PAGE

APPENDIX B
ERROR ANALYSIS

A. GENERAL

The accuracy of the experimental data presented in this report is determined by the errors (or uncertainties) associated with each of the parameters involved in the determination of an experimental value. These errors are determined individually and then compounded according to the accepted statistical principles to ascertain an estimate of the total error to be associated with the experiment.

B. STANDARD DEVIATION IN SPECIFIC DOSE RATE

The specific dose rate at any point is determined by the following equation:

$$D = \frac{M A T}{10^3\ p\ c\ s\ t} \qquad \text{(B-1)}$$

where

D = specific dose rate (R/hr/curie/ft^2)

M = scale reading on the dosimeter charger-reader (μa)

A = area of simulated source field (ft^2)

T = temperature (^oR)

p = barometric pressure (in. Hg)

c = charger-reader calibration constant

t = exposure time (hours)

s = source strength (curies)

The error in any measurement of D is related to the errors in the components by the total differential of D or

$$\Delta D = \frac{\partial D}{\partial M}\Delta M + \frac{\partial D}{\partial A}\Delta A + \frac{\partial D}{\partial P}\Delta P + \frac{\partial D}{\partial c}\Delta c + \frac{\partial D}{\partial S}\Delta S + \frac{\partial D}{\partial t}\Delta t + \frac{\partial D}{\partial T}\Delta T. \qquad \text{(B-2)}$$

By evaluating the partial derivatives, Eq. (B-2) is equivalent to:

$$\Delta D = D\left[\frac{\Delta M}{M} + \frac{\Delta A}{A} + \frac{\Delta T}{T} - \frac{\Delta p}{p} - \frac{\Delta c}{c} - \frac{\Delta s}{s} - \frac{\Delta t}{t}\right] \qquad (B-3)$$

The expected standard deviation (σ_D) of any [illegible] of many measurements of D is related to the standard deviations of its [illegible]ent parts by

$$\sigma_D = D\left[\left(\frac{\sigma_M}{M}\right)^2 + \left(\frac{\sigma_A}{A}\right)^2 + \left(\frac{\sigma_T}{T}\right)^2 + \left(\frac{\sigma_p}{p}\right)^2 \quad \left(\frac{\sigma_c}{c}\right)^2 + \left(\frac{\sigma_s}{s}\right)^2 + \left(\frac{\sigma_t}{t}\right)^2\right]^{1/2} \qquad (B-4)$$

When all of the parameters on the right side are independent of one another, it is often more convenient to speak of the error in terms of a fractional standard deviation.

Thus:

$$\frac{\sigma_D}{D_M} = \frac{D}{D_M}\left[\left(\frac{\sigma_M}{M}\right)^2 + \left(\frac{\sigma_A}{A}\right)^2 + \left(\frac{\sigma_T}{T}\right)^2 + \left(\frac{\sigma_p}{p}\right)^2 + \left(\frac{\sigma_c}{c}\right)^2 + \left(\frac{\sigma_s}{s}\right)^2 + \left(\frac{\sigma_t}{t}\right)^2\right]^{1/2} \qquad (B-5)$$

where D_M is the mean reading of D

Generally D/D_M should be small and may be assumed approximately equal to 1.

C. MEASUREMENT ERRORS.

The errors in the individual variables which together yield a specific dose rate have been measured or estimated as follows: (Reference 1)

---

1. An Experimental Evaluation of Roof Reduction Factors, by C. H. McDonnell, J. Velletri, PSDC-TR-16

1. Microamp Reading - The standard deviation of the microamp reading on the charger-reader has been found to consist of two components:

   a) Scale reading error: 0.5 μA
   b) Normal measured dosimeter group variation (see Appendix C): 1.0 μa.

   Thus σ_M is estimated to be approximately 1.0 μa as the scale reading error is included in this dosimeter variation.

2. Simulated Source Area - Extreme care was taken in laying out the tubing to simulate radiation fields. The error is thus believed to be quite small. A value of $\frac{\sigma_A}{A}$ of 0.001 (0.1 percent) has been assumed as typical.

3. Absolute Temperature - The largest source of error in determing a temperature at which an experiment was run is due to the variation of temperature with time during the course of an exposure. The total error in temperature, consists of two components, scale reading error and time variation of temperature during the experiment. The standard deviation of this value, σ_T is estimated to be approximately 3°R.

4. Barometric Pressure - Similarly, a small error is introduced by the time variation and scale reading error of the barometric pressure. These are assumed to be of approximately equal magnitude. The standard deviation σ_p is thus estimated to be 0.014 in. Hg.

5. Charger-Reading Calibration Constant - The charger-readers used in the experiments are calibrated as carefully and often as possible. Certain errors, however, are inherent in the calibration of the instruments and the calculation of the calibration constant. By close observation of the results of the calibration of various charger-readers with various types of dosimeters, it has been found that $\sigma_{c/c}$ is approximately equal to 0.035 or 3.5 percent.

6. Source Strength - All the sources were calibrated using NBS-calibrated Victoreen chambers and charger-readers. In addition to small errors in these instruments, there are also errors introduced by the measurement of source-to-detector distances and air density determinations. It has been estimated that an error of 2 percent ($\sigma_s / s = 0.02$) is to be associated with the source strength measurement.

7. Exposure Time - Measurement of the time in which the source is exposed is done with a stopwatch. The error induced is primarily that of reaction. For any given run, σ_t is estimated to be 1.0 second or 0.00028 hour.

D. SUMMARY OF INDIVIDUAL ERRORS

A summary of the individual errors follows:

Microamp reading:	σ_M	= 1 ua
Source area:	$\sigma_{A/A}$	= 0.001
Absolute temperature:	σ_T	= 3°R
Barometric pressure:	σ_p	= 0.014 in. Hg.
Calibration constant:	σ_c / c	= 0.035
Source strength:	σ_s / s	= 0.02
Exposure time:	σ_t	= 0.00028 hour.

Thus, for any experiment, equation (B-5) reduces to:

$$\frac{\sigma_D}{D_M} = \frac{D}{D_M}\left[\left(\frac{1}{M}\right)^2 + (0.001) + \left(\frac{3}{T}\right)^2 + \left(\frac{0.014}{p}\right)^2 + (0.035)^2 + (.02)^2 + \left(\frac{0.00028}{t}\right)^2\right]^{1/2}$$

or

$$\frac{\sigma_D}{D_M} = \frac{D}{D_M}\left[0.001626 + \left(\frac{1}{M}\right)^2 + \left(\frac{3}{T}\right)^2 + \left(\frac{0.014}{p}\right)^2 + \left(\frac{0.00028}{t}\right)^2\right]^{1/2} \quad \text{(B-6)}$$

These errors are the same for all experimental values throughout this report. It is felt that they accurately reflect the range within which at least 68.2 percent of the average value lie.

E. ERROR ASSOCIATED WITH SPECIFIC DOSE RATE FROM UNATTENUATED ROOF SOURCES

With each experimental exposure to determine dose rates within the structure, measurements were also made above the structure. This procedure provided unattenuated dose rates at various source-to-detector distances on the axis defining the centerline of the source field. Many variations were necessarily noticed in the individual parameters of Eq. (B-6).

The error measurement described above was performed on many of these points and the following are offered as examples of the use of the method of calculating $\frac{\sigma_D}{D_M}$:

1. Full Roof Source

Z = 8 feet above source

M =	50 μA	$\frac{1}{M}$	=	0.02
T =	510 °R	$\frac{3}{T}$	=	0.00588
p =	29.78 in. Hg	$\frac{0.014}{p}$	=	0.00047
t =	0.27 hour	$\frac{0.00028}{t}$	=	0.001037

D = 77.93 R/(hr/curie/ft^2)

D_M = 78.5 R/(hr/curie/ft^2)

$$\frac{\sigma_D}{D_M} = \frac{77.93}{78.5}\left[0.001626 + (.02)^2 + (0.00588)^2 + (0.00047)^2 + (0.001037)^2\right]^{1/2}$$

$$\frac{\sigma_D}{D_M} = 0.0451 = 4.51 \text{ per cent}$$

2. Diameter Circle (11.5 feet)

Z = 8 feet above source

M =	38 μ a	$\frac{1}{M}$	=	0.0263
T =	508°R	$\frac{3}{T}$	=	0.0059
p =	29.55 in. Hg	$\frac{0.014}{p}$	=	0.00045

$t = 0.0897$ hr $\qquad \frac{0.00028}{t} = 0.00312$

$D = 21.63$ hr/ curie/ ft^2

$D_M = 21.6$ hr/ curie/ ft^2

$$\frac{\sigma_D}{D_M} = \frac{21.63}{21.6}\left[0.001626 + (0.0263)^2 + (0.0059)^2 + (0.00045)^2 + (.00312)^2\right]^{1/2}$$

$$= 0.0487 = 4.87 \text{ percent}$$

The mean dose rate, D_M, was found by fitting a smooth curve through the experimental values obtained. As was mentioned above, this error analysis was performed on many experimental values and, from observation of these results, it seems reasonable to attribute a fractional error of $\sigma_D / D_M = 0.05$ (or 5 percent) to all unattenuated gamma dose rates resulting from the sources that were placed on the roof of the structure.

F. ERROR IN CONCRETE THICKNESS

The standard deviation of the concrete panels used in this series of experiments has been determined to be about 1.3 percent[2] of the nominal value of the concrete thickness. To determine a simple, but reasonably accurate method for estimating the effect of the concrete thickness error on the total specific dose rate within the structure, certain approximations were made. The dose rate beyond a concrete slab of thickness, x is related approximately to the unattenuated dose rate by the equation:

$$D(x) = D(0)\, e^{-\mu x} \qquad (B-7)$$

where:

$D(x)$ = attenuated dose rate within the structure (R/hr/curie/ft^2)

$D(0)$ = unattenuated dose rate (R/hr/curie/ft2)

2. Experimental Calibration and Analysis of the Radiation Test Facility at the Protective Structures Development Center, by C. H. McDonnell et al, PSDC-TR-14 (September 1964)

μ = linear attenuation coefficient ($(\text{length})^{-1}$)

x = concrete thickness (units of length).

Note that buildup within the concrete and the geometrical effects of the structure and the source field have been neglected. This is a fair assumption since the slope of the attenuated dose rate does approximate an exponential of this type.

The total differential of D(x) is:

$$\Delta D(x) = \frac{\partial D(x)}{\partial D(0)} \quad \Delta D(0) \quad + \quad \frac{\partial D(x)}{\partial x} \quad \Delta x$$

or

$$\Delta D(x) = e^{-\mu x} \Delta D(0) - \mu D(0) e^{-\mu x} \Delta x$$

This is equivalent to

$$\frac{\Delta D(x)}{D(x)} = \frac{\Delta D(0)}{D(0)} - \mu \Delta x$$

In terms of fractional error this becomes

$$\frac{\sigma_{D(x)}}{D(x)} = \left[\left(\frac{\sigma_{D(0)}}{D(0)} \right)^2 + \left(\mu x \frac{\sigma_x}{x} \right)^2 \right]^{1/2} \qquad \text{(B-8)}$$

where μx equals the number of mean free paths in the concrete between the source and the detector. The quantity $\sigma_{D(0)}/D(0)$ is the same quantity as previously evaluated (see Eq. (B-5). The standard deviation of concrete thickness expressed as a fractional error σ_x / x which, as mentioned above, was found to be 0.013.

Thus if a conservatively high value of $\sigma_{D(x)}/D_M = 0.05$ is assumed, Eq. (B-8) becomes:

$$\frac{\sigma_{D(x)}}{D_{(x)}} = \left[0.0025 + \left(\mu x \frac{\sigma_x}{x} \right)^2 \right]^{1/2} \qquad \text{(B-9)}$$

where

R_f = roof reduction factor

$D(x)$ = specific dose rate within the structure (R/hr/curie/ft^2)

D_o = infinite field dose rate (R/hr/curie/ft^2)

Therefore

$$\Delta R = \frac{\partial R}{\partial D(x)} \quad \Delta D(x) + \frac{\partial R}{\partial D_o} \quad \Delta D_o$$

or equivalently

$$\frac{\Delta R}{R} = \frac{\Delta D(x)}{D(x)} - \frac{\Delta D_o}{D_o} \qquad \text{(B-11)}$$

In terms of fractional error:

$$\frac{\sigma_R}{R} = \left[\left(\frac{\sigma_{D(x)}}{D(x)} \right)^2 + \left(\frac{\sigma_{Do}}{D_o} \right)^2 \right]^{1/2}$$

σ_{Do}/D_o is equal to 0.03685 and $\sigma Dx/Dx$ is dependent on the thickness of concrete between source and detector. Thus:

$$\frac{\sigma_R}{R} = \left[\left(\frac{\sigma_{D(x)}}{D(x)} \right)^2 + 0.001358 \right]^{1/2}$$

The total fractional error inherent in the roof reduction factor as a function of concrete thickness is presented below:

2. Experimental Calibration and Analysis of the Radiation Test Facility at the Protective Structures Development Center, by C. H. McDonnell, etal, PSDC-TR-14 (September 1964).

1. An Experimental Evaluation of Roof Reduction Factors, by C. H. McDonnell, J. Velletri, PSDC-TR-16 (May 1966).

In the experiments performed, the total concrete thicknesses varied from 4 to 24 inches, depending on which structure was under investigation and on which floor the detector in question was located. The standard deviations, expressed as fractional errors in the specific dose for all of the concrete thicknesses used, are calculated below:

x (in.)	μx	$\left(\mu x \frac{\sigma_x}{x}\right)^2$	$\frac{\sigma_{D(x)}}{D(x)}$
0	0	0	0.050
4	1.34	0.000303	0.053
8	2.68	0.001214	0.061
12	4.02	0.002731	0.072
16	5.36	0.004855	0.086
24	8.04	0.010924	0.116

Thus, while there can be no single error attributed to the specific dose rate in the structure caused by roof sources, a single error may be associated with each floor thickness under consideration.

G. APPLICATION OF ERROR ANALYSIS TO ROOF REDUCTION FACTORS

Most of the results of the experimental roof programs in this report have been presented as roof reduction factors. The roof reduction factor is defined as the ratio of the dose rate at any point in the structure caused by contaminated field on the roof to the dose rate at a point 3 feet above the ground caused by an infinite plane source of contamination. The infinite field value D_o has been measured in previous experiments[2] to have a value of 464 R/hr/curie/ft^2. There is a fractional error of $\sigma Do/D_o = 0.03685$ associated with this value. The evaluation of $^{\sigma}Do/D_o$ can be found in Reference 1, with a slight change in the final value caused by a later calculation of the calibration constant error.

The calculation of $^{\sigma}Do/D_o$ includes the error associated with a ground roughness correction which is necessary because the experimental measurement was of necessity conducted on other than a mathematically smooth plane. The total fractional error in the roof reduction factor may be found by starting with the definition of such a roof reduction factor:

$$R_f = \frac{D(x)}{D_o} \qquad (B-10)$$

x (in.)	$\sigma_{D(x)} / D(x)$	σ_{R_f} / R_f
0	0.05	0.062
4	0.053	0.065
8	0.061	0.071
12	0.072	0.081
16	0.086	0.094
24	0.116	0.122

The standard deviation in the roof reduction factor is found by multiplying the reduction factor at the point in question by the appropriate σ_{R_f} / R_f

H. EXPERIMENTAL VERIFICATION OF ERROR ANALYSIS

The error analysis presented above is based on estimates of errors or uncertainties in the instruments used and other parameters associated with determining an experimental value of the gamma dose rate. The experiments conducted at the Protective Structures Development Center are repeated many times for each structural configuration so that a variety of points are available to yield a mean value of the dose rate at any particular position. Figure B-1 shows typical examples of the various experimental points taken on two floors of a structure together with the mean value of the dose rate and the limits of the error band predicted by the above error analysis in attenuated dose rate. The derived band of error or uncertainty seems to be quite good in predicting experimental error.

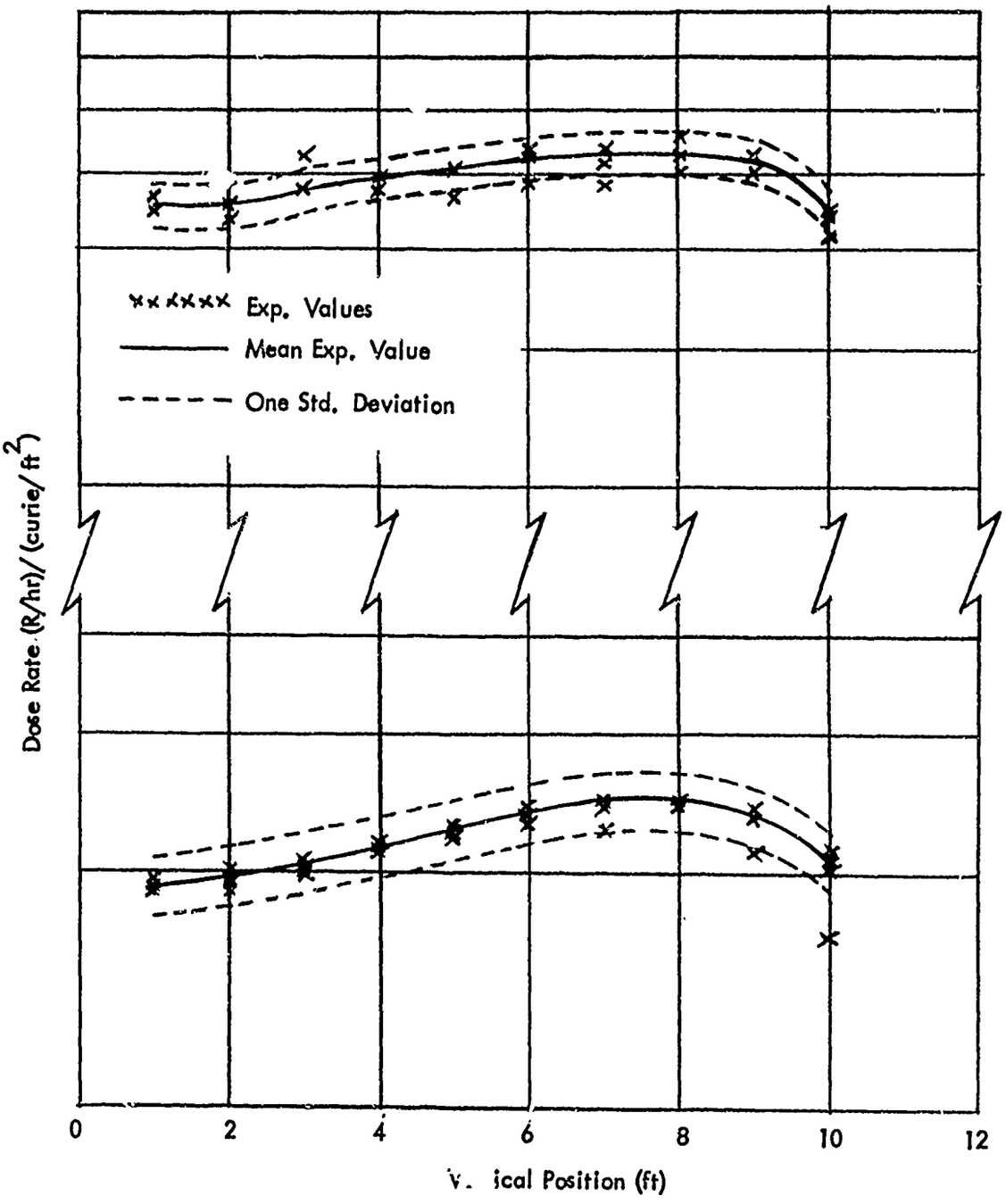

FIG. B-1 - Typical Repeated Data and Error Band

APPENDIX C

EXPERIMENTAL DATA

Presentation of results as roof reduction factors assumes a measured value of the dose encountered at a point 3 feet in the air above an infinite, uniformly contaminated plane of radiation. At the Protective Structures Development Center, this value has been measured to be 464 R/hr/curie/ft^2. A detailed description of the measurement of this specific dose rate is presented in Reference 1.

Measurements of the gamma dose within the structure for the series of experiments analyzed in this report were made with Victoreen Model 362 (200 mr), Model 229 (10 mr), and Model 208 (1 mr), non-direct reading ionization chambers (dosimeters) together with a Technical Operation Model 556 charger-reader. Selection of a particular dosimeter for any specific experiment was based on the dose expected at the detector location from a particular source, source field, exposure time, and concrete thickness between source and detector.

The dosimeters used and the charger-reader were calibrated before use in the experiments against a gamma source of known strength and Victoreen R meters calibrated by the National Bureau of Standards. The only dosimeters used in the experiments were those which responded to within ± 2 percent of the known dose. At various times during the experiments, a secondary calibration was performed on the instruments to check the agreement of the dosimeters with each other.

Two Co-60 gamma sources were utilized in this set of experiments. These sources had values of 4.14 and 41.4 curies on January 2, 1966.

The dosimeter readings were all normalized to specific dose rates in roentgens per hour for a source density of 1 curie of Co-60 per square foot of source plane area. This is accomplished by means of the following equation:

$$D_s = \frac{M A T}{10^3 \; p c s t} \qquad (C\text{-}1)$$

where:

D_s = specific dose rate R/hr/curie/ft^2

1. C. H. McDonnell, H. Velletri, An Experimental Evaluation of Roof Reduction Factors, PSDC-TR-16 (May 1966)

M = scale reading on the dosimeter charger-reader (μA)

A = area of simulated source field (ft^2)

T = temperature (^oR)

p = barometric pressure (in. Hg)

c = charger-reader calibration constant $\frac{\mu a}{R} \quad \frac{^oR}{in\text{-}Hg}$

t = exposure time (hours)

s = source strength (curies)

The specific dose rates measured in the experiments are tabulated in this Appendix. Table C-1 shows the centerline values as a function of source detector distance for both the full roof source and the 11.5 foot diameter circle for the four and eight inch floor cases. Tables C-2 and C-3 present similar values for the off-center positions.

TABLE C-1

SPECIFIC DOSE RATES, FULL ROOF SOURCE, AND DISK SOURCE
(R/hr/curie/ft^2)
Centerline Positions

Distance from source (ft)	48.6 psf Roof and floors		Distance from source (ft)	97.2 psf Roof and floors	
	Full Roof	11.5'dia. circle		Full Roof	11.5'circle
1.3	16.4	12.9			
2	20.7	16.7	2	4.50	4.2
3	21.4	15.8	3	5.20	4.25
4	21.2	14.5	4	5.30	4.04
5	21.3	11.3	5	5.30	3.52
6	20.1	9.57	6	5.23	2.96
7	19.0	7.90	7	5.03	2.54
8	18.4	6.60	8	4.92	2.20
9	17.5	5.83	9	4.76	1.90
10	16.7	4.91	10	4.55	1.66
11	16.0	4.45	11	4.54	1.46
14	3.18	0.730	14	0.206	0.0812
15	3.30	0.760	15	0.236	0.0835
16	3.25	0.705	16	0.246	0.0830
17	3.13	0.660	17	0.246	0.0760
18	2.97	0.580	18	0.238	0.0675
19	2.77	0.550	19	0.227	0.0625
20	2.66	0.509	20	0.215	0.0560
21	2.49	0.480	21	0.205	0.0516
22	2.38	0.447	22	0.197	0.0487
23	2.27	0.411	23	0.192	0.0440
25.33	0.364	0.0712			
26.33	0.442	0.0780	26.67	0.0112	-----
27.33	0.464	0.0770	27.67	0.0118	-----
28.33	0.467	0.0800	28.67	0.0118	-----
29.33	0.453	0.0722	29.67	0.0118	-----
30.33	0.435	0.0686	30.67	0.0109	-----
31.33	0.413	0.0645	31.67	0.0106	-----
32.33	0.402	0.0619	32.67	0.0103	-----
33.33	0.390	0.0608	33.67	0.0100	-----
34.33	0.408	0.0566	34.67	0.00916	-----
35.33	0.359	0.0542			

TABLE C-2

SPECIFIC DOSE RATES, FULL ROOF SOURCE

(r/hr/curie/ft^2)

Off Center Positions
48.6-psf floors

Position *	Distance from source (ft)								
X, Y	32.33	29.33	25.33	21	18	15	9	5	3
+10, +15	0.220	0.244	0.298	1.26	1.41	1.70	9.18	11.7	18.1
-10, +15	0.234	0.256	0.318	1.29	1.47	1.71	9.12	11.2	16.3
-10, -15	0.225	0.255	0.309	1.32	1.41	1.70	8.76	10.7	16.0
+10, -15	0.236	0.252	0.318	1.52	1.50	1.74	9.47	11.2	16.8
+6, +9	0.329	0.375	0.465	1.99	2.33	2.81	15.2	17.7	20.7
-6, +9	0.296	0.365	0.440	2.01	2.37	2.76	14.8	17.9	21.3
-6, -9	0.320	0.364	0.452	1.99	2.37	2.87	14.9	17.9	21.2
+6, -9	0.326	0.375	0.460	2.02	2.37	2.88	15.0	17.6	21.3
0, +15	0.310	0.341	0.353	1.71	2.06	2.31	12.9	15.7	20.2
0, -15	0.302	0.333	0.352	1.68	2.02	2.35	12.5	15.3	19.5
0, +9	0.348	0.395	-----	2.16	2.46	2.79	16.5	18.9	21.4
0, -9	0.348	0.393	-----	-----	-----	-----	16.1	-----	21.0
+6, 0	0.372	0.432	0.515	2.23	2.72	3.13	15.9	18.4	21.3
-6, 0	0.366	0.423	0.504	2.19	2.76	3.32	16.1	18.7	21.8
+10, 0	0.311	0.348	0.425	1.77	2.11	2.47	12.5	14.2	18.6
-10, 0	0.318	0.360	0.447	1.83	2.10	2.55	12.5	14.3	18.9

*See Figure 3.4

TABLE C-3

SPECIFIC DOSE RATES, FULL ROOF SOURCE

(R/hr/curie/ft^2)

Off Center Positions
97.2-psf floors

Position *	Distance from Source (ft)					
X, Y	21	18	15	9	6	3
+10, +15	------	0.108	0.143	2.65	3.40	5.20
-10, +15	0.090	0.102	0.131	2.42	3.11	4.63
-10, -15	0.102	0.102	0.137	2.40	3.11	4.50
+10, -15	0.096	0.102	0.137	2.38	3.04	4.45
+6, +9	0.167	0.195	0.260	4.00	4.60	5.40
-6, +9	0.165	0.193	0.231	3.96	4.50	5.25
-6, -9	0.163	0.193	0.236	3.97	4.61	5.40
+6, -9	0.159	0.190	0.225	4.04	4.63	5.60
0, +15	0.154	0.166	0.190	3.58	4.10	5.20
0, -15	0.143	0.161	0.178	3.40	4.02	4.95
0, +9	0.178	0.207	0.231	4.24	4.80	5.15
0, -9	0.178	0.207	0.231	4.24	4.62	5.00
+6, 0	0.184	0.212	0.242	4.12	4.77	5.41
-6, 0	0.178	0.212	0.254	4.20	4.90	5.50
+10, 0	0.143	0.161	0.178	3.42	4.00	4.96
-10, 0	0.143	0.172	0.196	3.34	3.82	5.03

*See Figure 3.4

UNCLASSIFIED
Security Classification

DOCUMENT CONTROL DATA - R&D

(Security classification of title, body of abstract and indexing annotation must be entered when the overall report is classified)

1 ORIGINATING ACTIVITY *(Corporate author)*
Protective Structures Development Center
7809 Telegraph Road, Building 2590, Alexandria, Va. 22310

2a. REPORT SECURITY CLASSIFICATION
UNCLASSIFIED

2b. GROUP

3. REPORT TITLE
AN EXPERIMENTAL EVALUATION OF ROOF REDUCTION FACTORS WITHIN A MULTI-STORY BUILDING

4. DESCRIPTIVE NOTES *(Type of report and inclusive dates)*
Final Report

5. AUTHOR(S) *(Last name, first name, initial)*
Spring, R. and McDonnell, C.

6. REPORT DATE	7a. TOTAL NO. OF PAGES	7b. NO. OF REFS
April 1967	49	10

8a. CONTRACT OR GRANT NO.

b. PROJECT NO.
OCD-PS-65-17, OCD Subtask 1117A

c.
(OCD) DAHC20-67-W-0111, OCD Subtask 1117A

d.

9a. ORIGINATOR'S REPORT NUMBER(S)
PSDC-TR-16, Supplement No. 1

9b. OTHER REPORT NO(S) *(Any other numbers that may be assigned this report)*

10. AVAILABILITY/LIMITATION NOTICES
Distribution of this document is unlimited

11. SUPPLEMENTARY NOTES

12. SPONSORING MILITARY ACTIVITY
Department of the Army
Office of the Secretary of the Army
Office of Civil Defense

13. ABSTRACT

Fallout contamination deposited on the roof of a structure is, in many cases, the source of the primary radiation component of the total dose obtained at any point within the structure. Experiments have been performed in which the doses from a source of radiation present on a roof were measured in many locations within a multi-story building.

This report presents the results of these experiments for roof and floor mass thicknesses of 48.6 and 97.2 psf. Comparisons of the experimentally measured gamma doses with those determined theoretically have been shown throughout this report. Agreement between experiment and theory has, in general, been found to be good.

DD FORM 1 JAN 64 1473

UNCLASSIFIED
Security Classification

UNCLASSIFIED
Security Classification

14. KEY WORDS	LINK A		LINK B		LINK C	
	ROLE	WT	ROLE	WT	ROLE	WT
Roof attenuation - gamma radiation Radiation shielding Concrete attenuation - gamma radiation Co-60						

INSTRUCTIONS

1. ORIGINATING ACTIVITY: Enter the name and address of the contractor, subcontractor, grantee, Department of Defense activity or other organization *(corporate author)* issuing the report.

2a. REPORT SECURITY CLASSIFICATION: Enter the overall security classification of the report. Indicate whether "Restricted Data" is included. Marking is to be in accordance with appropriate security regulations.

2b. GROUP: Automatic downgrading is specified in DoD Directive 5200.10 and Armed Forces Industrial Manual. Enter the group number. Also, when applicable, show that optional markings have been used for Group 3 and Group 4 as authorized.

3. REPORT TITLE: Enter the complete report title in all capital letters. Titles in all cases should be unclassified. If a meaningful title cannot be selected without classification, show title classification in all capitals in parenthesis immediately following the title.

4. DESCRIPTIVE NOTES: If appropriate, enter the type of report, e.g., interim, progress, summary, annual, or final. Give the inclusive dates when a specific reporting period is covered.

5. AUTHOR(S): Enter the name(s) of author(s) as shown on or in the report. Enter last name, first name, middle initial. If military, show rank and branch of service. The name of the principal author is an absolute minimum requirement.

6. REPORT DATE: Enter the date of the report as day, month, year, or month, year. If more than one date appears on the report, use date of publication.

7a. TOTAL NUMBER OF PAGES: The total page count should follow normal pagination procedures, i.e., enter the number of pages containing information.

7b. NUMBER OF REFERENCES: Enter the total number of references cited in the report.

8a. CONTRACT OR GRANT NUMBER: If appropriate, enter the applicable number of the contract or grant under which the report was written.

8b, 8c, & 8d. PROJECT NUMBER: Enter the appropriate military department identification, such as project number, subproject number, system numbers, task number, etc.

9a. ORIGINATOR'S REPORT NUMBER(S). Enter the official report number by which the document will be identified and controlled by the originating activity. This number must be unique to this report.

9b. OTHER REPORT NUMBER(S). If the report has been assigned any other report numbers *(either by the originator or by the sponsor)*, also enter this number(s).

10. AVAILABILITY/LIMITATION NOTICES: Enter any limitations on further dissemination of the report, other than those imposed by security classification, using standard statements such as:

(1) "Qualified requesters may obtain copies of this report from DDC."

(2) "Foreign announcement and dissemination of this report by DDC is not authorized."

(3) "U. S. Government agencies may obtain copies of this report directly from DDC. Other qualified DDC users shall request through _____."

(4) "U. S. military agencies may obtain copies of this report directly from DDC. Other qualified users shall request through _____."

(5) "All distribution of this report is controlled. Qualified DDC users shall request through _____."

If the report has been furnished to the Office of Technical Services, Department of Commerce, for sale to the public, indicate this fact and enter the price, if known.

11. SUPPLEMENTARY NOTES: Use for additional explanatory notes.

12. SPONSORING MILITARY ACTIVITY: Enter the name of the departmental project office or laboratory sponsoring *(paying for)* the research and development. Include address.

13. ABSTRACT. Enter an abstract giving a brief and factual summary of the document indicative of the report, even though it may also appear elsewhere in the body of the technical report. If additional space is required, a continuation sheet shall be attached.

It is highly desirable that the abstract of classified reports be unclassified. Each paragraph of the abstract shall end with an indication of the military security classification of the information in the paragraph, represented as *(TS)*, *(S)*, *(C)*, or *(U)*.

There is no limitation on the length of the abstract. However, the suggested length is from 150 to 225 words.

14. KEY WORDS: Key words are technically meaningful terms or short phrases that characterize a report and may be used as index entries for cataloging the report. Key words must be selected so that no security classification is required. Identifiers, such as equipment model designation, trade name, military project code name, geographic location, may be used as key words but will be followed by an indication of technical context. The assignment of links, rules, and weights is optional.

UNCLASSIFIED
Security Classification